Surv Geophys (2015) 36:483–511
DOI 10.1007/s10712-015-9315-5

Unexpected Very Low Frequency (VLF) Radio Events Recorded by the Ionospheric Satellite DEMETER

M. Parrot · J. J. Berthelier · J. Blecki · J. Y. Brochot · Y. Hobara · D. Lagoutte · J. P. Lebreton · F. Němec · T. Onishi · J. L. Pinçon · D. Píša · O. Santolík · J. A. Sauvaud · E. Slominska

Received: 26 September 2014 / Accepted: 10 January 2015 / Published online: 12 February 2015
© Springer Science+Business Media Dordrecht 2015

Abstract DEMETER was a low Earth orbiting microsatellite in operation between July 2004 and December 2010. Its scientific objective was the study of ionospheric perturbations in relation to seismic activity and man-made activities. Its payload was designed to measure electromagnetic waves over a large frequency range as well as ionospheric plasma parameters (electron and ion densities, fluxes of energetic charged particles). This paper will show both expected and unusual events recorded by the satellite when it was in operation. These latter events have been selected from the DEMETER database because they are rare or even have never been observed before, because they have a very high intensity, or because they are related to abnormalities of the experiments under particular plasma conditions. Some events are related to man-made radio waves emitted by VLF ground-based transmitters or power line harmonic radiation. Natural waves, such as atypical quasi-periodic emissions or uncommon whistlers, are also shown.

M. Parrot (✉) · J. Y. Brochot · D. Lagoutte · J. P. Lebreton · J. L. Pinçon
LPC2E/CNRS, Orléans, France
e-mail: mparrot@cnrs-orleans.fr

J. J. Berthelier · T. Onishi
LATMOS/IPSL/UVSQ, Paris, France

J. Blecki · E. Slominska
CBK, Warsaw, Poland

Y. Hobara
UEC, Tokyo, Japan

F. Němec · O. Santolík
Faculty of Mathematics and Physics, Charles University in Prague, Prague, Czech Republic

D. Píša · O. Santolík
Institute of Atmospheric Physics AS CR, Prague, Czech Republic

J. A. Sauvaud
IRAP, Toulouse, France

Keywords Ionosphere · Natural and man-made VLF radio emissions · Anomalies

1 Introduction

DEMETER was a three-axis stabilized Earth-pointing spacecraft launched on June 29, 2004, into a low altitude ($\sim$710 km) polar orbit that was subsequently lowered to 650 km where it remained until the end of the mission in December 2010. The orbit was nearly Sun-synchronous with an ascending node at 22:30 LT in the night sector and a descending node at 10:30 LT during daytime. The main objectives of DEMETER were the search for ionospheric disturbances possibly generated by pre-seismic activity, the investigation of ionospheric effects of man-made activities and, more generally, the study of space weather and ionospheric phenomena. To achieve these aims, the scientific payload included a complete set of instruments to measure the electric and magnetic components of plasma waves and to monitor the main parameters of the ionospheric plasma.

The electric field instrument (ICE) measured the three electric components of plasma waves in the frequency range from D.C. to 3.25 MHz. The very low frequency (VLF) range of ICE extends from 70 Hz to 20 kHz and the high-frequency (HF) range from 10 kHz to 3.25 MHz. The magnetic field experiment (IMSC) measured the three magnetic components in the frequency range from 10 Hz to 20 kHz. There were two scientific modes, Survey and Burst, this latter mode being mainly activated when the satellite was above active seismic regions or for specific purposes. Survey mode data provided the 2.048-s-averaged VLF power spectra of one electric component and one magnetic component with a frequency resolution of 19.5 Hz, and the 2.048-s-averaged HF spectra of the same electric component with a frequency resolution of 3.25 kHz. In the Burst mode, the VLF waveforms of the same electric field component and the same magnetic component were simultaneously recorded. The electron density was measured by a Langmuir probe named ISL with a resolution of 1 s and the ion density and composition were provided by a retarding potential analyzer with a resolution of $\sim$4 s. All experiments are fully described in the special issue of *Planetary and Space Sciences* published in April 2006.

DEMETER recorded data all around the Earth except in the auroral zones because this part of the orbit was used to maintain the satellite attitude (Cussac et al. 2006). Consequently, no data have been recorded when the invariant latitude is larger than 65°, except from time to time to allow conjunctions with HAARP or EISCAT experiments which have been used to heat the ionosphere with HF waves (see, for example, Piddyachiy et al. 2008). Between July 2004 and December 2010, DEMETER continuously recorded data except for some periods. From September 20, 2005, until October 20, 2005, the satellite was used by a CNES technical experiment for autonomous orbit control (as was also the case for some orbits during the mission). From time to time, the satellite went in a safe mode due to single-event upsets (SEUs) or because the stellar sensor was dazzled by the full moon. A few days were then necessary to recover the normal situation. During rare occasions, SEUs also produced troubles in the electronics of the wave experiment. They were suppressed by a reset which was automatic when the mode changed (Survey to Burst or Burst to Survey) and, of course, when the experiment was switched off at the end of a half-orbit. A list of the orbits with trouble in the data is available from the authors.

In addition to the planned data handling (Lagoutte et al. 2006), all the VLF waveforms of one electric component recorded during the Burst mode have been automatically

processed in order to produce spectrograms with high time (0.1 s) resolution and good frequency (9.7 Hz) resolution. Plots with durations of 2 min have been stored in a database and most of the spectrograms shown in this paper are extracted from this database. The aim of this paper was to show unusual events recorded by DEMETER in relation to different man-made activities (Sects. 2, 3), and with natural phenomena linked to magnetic storms (Sects. 4, 5) or thunderstorms (Sect. 6). Sections 7 and 8 are devoted to problems of the ICE experiment in specific plasma conditions or orbital configurations, whereas Sect. 9 reports uncommon interferences. The conclusions of this research are given in Sect. 10.

2 VLF Radio Transmitters

Ground-based VLF radio transmitters are used by the navies of different countries to communicate with submarines. These transmitters emit a continuous wave at a fixed frequency or pulse as is the case for the three α transmitters in Russia. It has been shown that they significantly perturb the ionospheric density (Parrot et al. 2007; Bell et al. 2011) and that they contribute to the precipitation of energetic charged particles from the Van Allen radiation belts (Sauvaud et al. 2008; Clilverd et al. 2008; Bell et al. 2008; Gamble et al. 2008; Li et al. 2012). In the VLF spectrograms, they usually appear as horizontal thin lines with a constant frequency. However, sometimes during the traversing of a disturbed ionosphere a large frequency broadening of the signal occurs. This has been well observed and studied in the past with other satellites (see for example Bell et al. 1981 and Titova et al. 1984). Such observations are also common with DEMETER, but particularly strong broadening has been observed; Fig. 1 shows two examples related to the α transmitter pulses. These transmitters emit signals at three different frequencies between 11 and 15 kHz and Fig. 1 illustrates how the broadening can take different forms. The left spectrogram of Fig. 1 is related to data recorded on April 14, 2006, between 16:16:30 and 16:18:30 UT. It can be seen that very strong electrostatic noises are associated with each pulse, whereas in the right spectrogram of Fig. 1, which is related to data recorded on March 23, 2005, between 06:36:00 and 06:38:00 UT, the shapes of the pulses are completely distorted.

The broadening of the VLF transmitter signals is not always due to the ionosphere and many events have been observed by DEMETER where the transmitter intentionally radiates over a large bandwidth. Two examples are shown in Fig. 2 for data recorded on December 18, 2005, between 02:51:00 and 02:53:00 UT (left) and for data recorded on December 19, 2006, between 04:02:30 and 04:04:30 UT (right). In these two spectrogram panels, one can observe a broadband signal centered on 17.8 kHz. For the event shown in the right spectrogram, the signal is normal at the beginning, then there is a period where the transmitter is switched off, and at the end there is a broadband frequency signal. This is due to tests done by the US army from an aircraft. All these events are observed above the USA or above the corresponding magnetically conjugate region (see the maps below the spectrograms).

Figure 3 shows examples of spurious lines induced by VLF ground-based transmitters in Europe. They are indicated by a curly bracket between 0 and 5 kHz. They appear when the transmitter signals received by the satellite have a broadband frequency due to a disturbed ionosphere (Bell et al. 2011). There are several powerful transmitters in Europe, and these lines between 0 and 5 kHz are due to beating of the frequencies of the different transmitters. This may be induced by saturation in the electronics. All these events are observed above Europe and in the conjugate area close to South Africa (see the map below the spectrogram).

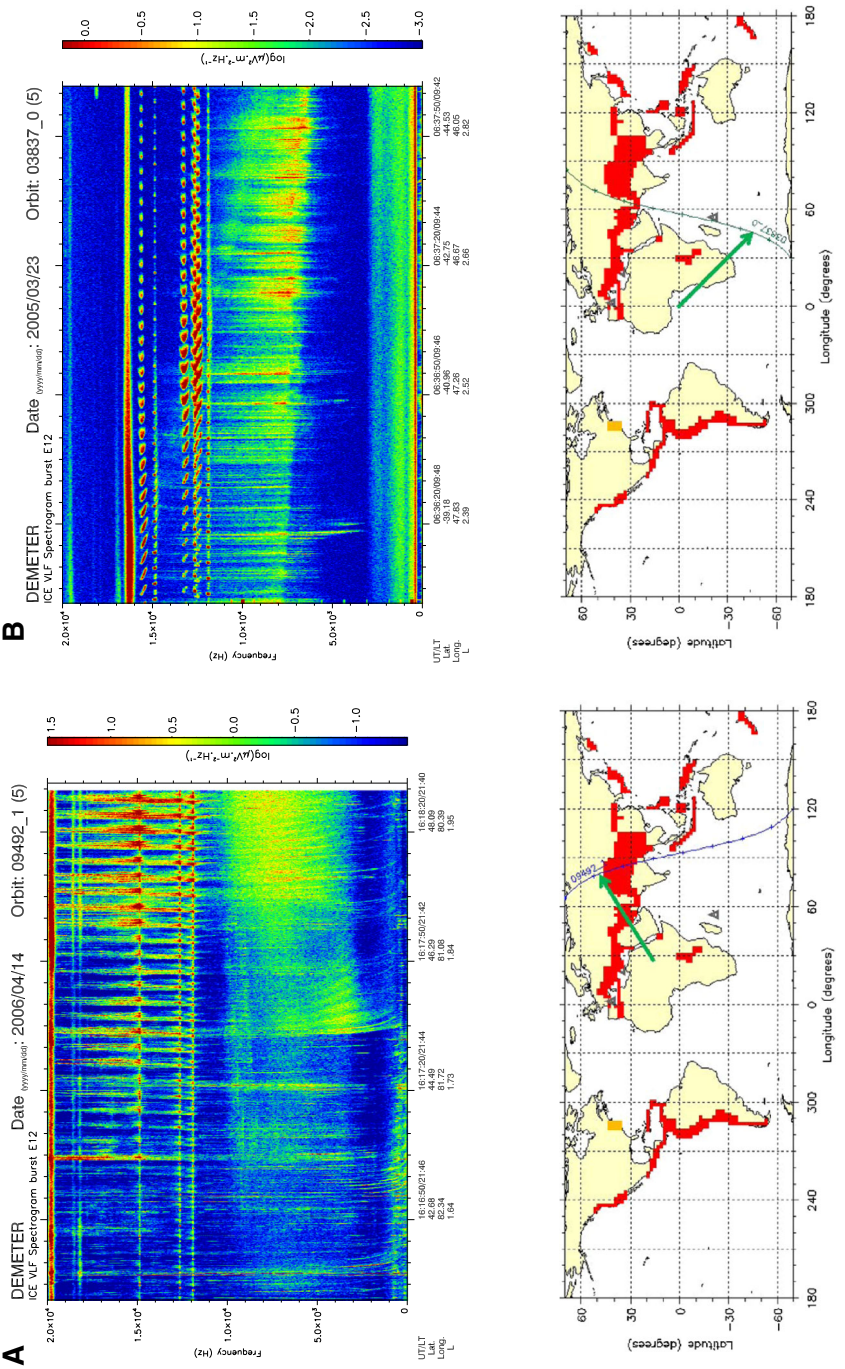
A
DEMETER
ICE VLF Spectrogram burst E12
Date (yyyy/mm/dd) : 2006/04/14
Orbit: 09492_1 (5)
Frequency (Hz)
log(μV².m⁻².Hz⁻¹)
B
DEMETER
ICE VLF Spectrogram burst E12
Date (yyyy/mm/dd) : 2005/03/23
Orbit: 03837_0 (5)
Frequency (Hz)
log(μV².m⁻².Hz⁻¹)
Latitude (degrees)
Longitude (degrees)
09492_1
03837_0

◀**Fig. 1** VLF spectrograms of an electric field component in the frequency range 0–20 kHz showing frequency broadening of the pulses from the α VLF transmitter located at Novosibirsk (55°45′N, 84°26′E) due to their traversing the ionosphere. In the left spectrogram data were recorded on April 14, 2006, between 16:16:30 and 16:18:30 UT close to the transmitter. In the right spectrogram data were recorded on March 23, 2005, between 06:36:00 and 06:38:00 UT in the opposite hemisphere. The intensity is color-coded according to the scale on the right. At the bottom of each panel, the universal time, the local time, the geographic latitude and longitude (positive latitudes correspond to the northern hemisphere, whereas negative latitudes are related to the southern hemisphere; longitude varies from 0° to 360°), and the L parameter of McIlwain (1961) are shown. Each spectrogram is associated with a map of the Earth showing the corresponding half-orbit and the location of the event (*green arrow*). On this map, the *red areas* indicate the main locations of the Burst mode. Some frequency lines related to other transmitters can be identified in the spectrograms [19.8 kHz due to NWC (21°48′S, 114°09′E); 18.6 kHz due to NTS (38°28′S, 146°56′E; 18.3 kHz due to HWU (46°42′N, 001°14′E); 16.2 kHz due to UBE (52°55′N, 158°39′)]. Each *vertical line* is a whistler which corresponds to a lightning stroke in the atmosphere

A VLF transmitter signal with an unusually low frequency is shown in Fig. 4. The data were recorded on August 18, 2008, between 04:16:20 and 04:18:00 UT when the satellite was above China. The frequency of the transmitter is 5 kHz, and the signal is formed of pulses of 0.5 s duration. This transmitter has been observed several times by DEMETER, but irregularly.

When the satellite was close to the NLK transmitter (Jim Creek, USA), additional emissions were very often observed. An example is shown in Fig. 5 which concerns data recorded on March 18, 2009, between 05:26:00 and 05:28:00 UT. The frequency of NLK is 24.8 kHz, but the signal is so strong when the satellite is above the transmitter that there is an aliasing problem (even with the seventh order Chebyshev filters on the input) and in the spectrogram it appears at 15.2 kHz. One can observe a set of strange lines at harmonics of 1 kHz between 05:26:40 and 05:27:10 UT at frequencies up to 8 kHz. Their origin and their function are unknown.

Sometimes as the VLF radio transmitter signal traverses the ionosphere, sidebands are induced around the transmitter frequency. This sideband structure is due to an interaction with natural ELF emissions (Bell 1985; Tanaka et al. 1987; Sotnikov et al. 1991). These sidebands have also been observed by DEMETER and a very particular example is shown in Fig. 6. The corresponding spectrogram is related to data recorded on October 16, 2004, between 09:09:00 and 09:11:00 UT. It can be seen that there are several sidebands and that they are enhanced at some specific locations. This can be attributed to small-scale plasma variations along the path of the transmitter signal to the satellite. There are several events similar to this one in the DEMETER database.

3 PLHR and MLR

Power line harmonic radiation (PLHR) consists of ELF and VLF radio waves at the harmonic frequencies of 50 or 60 Hz radiated by electric power systems on the ground. Frequency–time spectrograms of these events typically consist of several horizontal lines with mutual separations of 50/100 or 60/120 Hz. Evidence of PLHR propagation in the magnetosphere was first obtained from ground-based observations (Helliwell et al. 1975). A systematic study of PLHR observations by the microsatellite DEMETER was performed by Němec et al. (2006, 2007b, 2008, 2010) (see also references to other observations therein). They showed that the frequency spacing of the lines corresponds well to the power system frequency in possible generation regions. Parrot et al. (2014a) investigated the emissions triggered by PLHR.

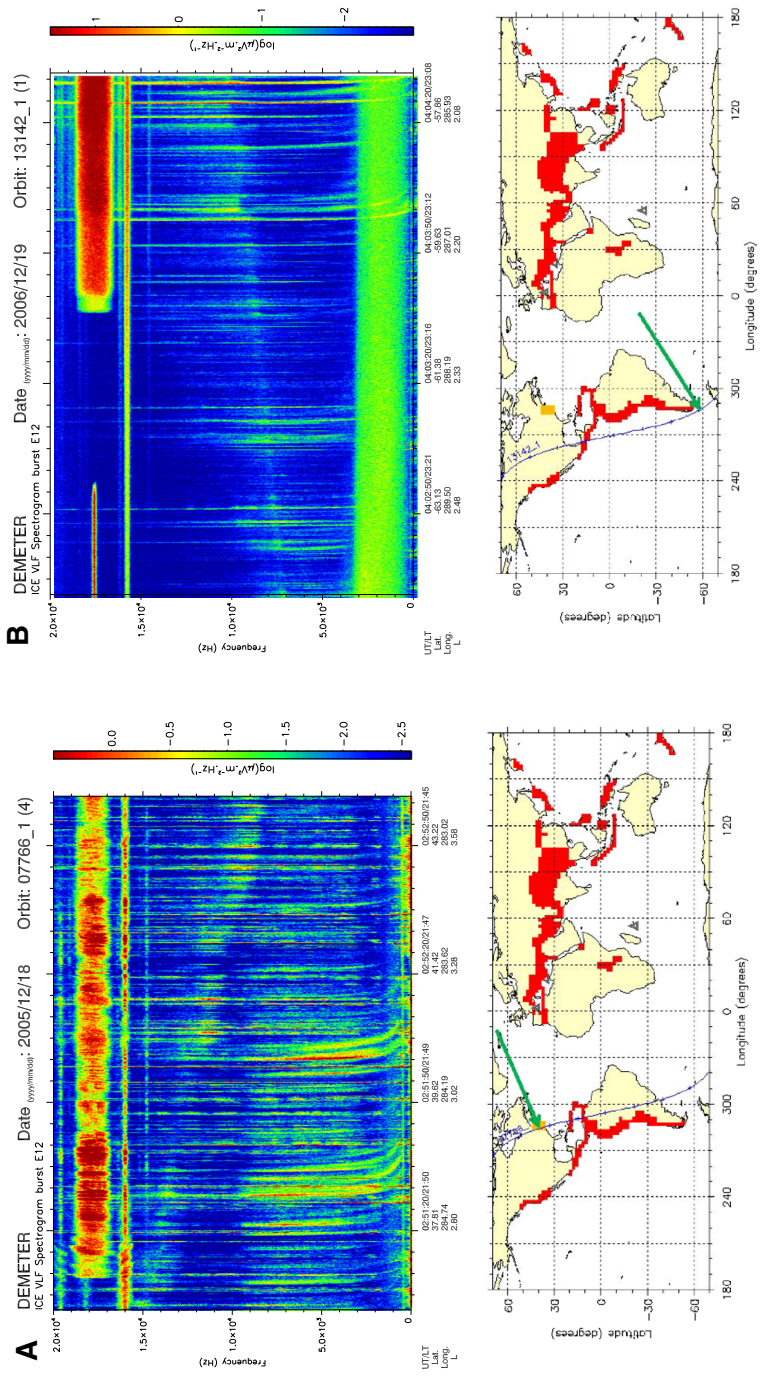

The event which is shown in Fig. 7 is remarkable because the PLHR is observed at very high frequencies. One can see in the spectrogram of Fig. 7 a set of 8 lines between 10 and 13 kHz. The two dashed lines are due to the pulses of the α transmitters (see Sect. 2). These eight lines are

◀**Fig. 2** (*Left*) Data recorded on December 18, 2005, between 02:51:00 and 02:53:00 UT; (*right*) data recorded on December 19, 2006, between 04:02:30 and 04:04:30 UT. The panel below each spectrogram shows the half-orbit and the location of the event. The two *spectrogram panels* show intentional spectral broadening of the frequency of the VLF transmitter around 17.8 kHz. This frequency and the 24 kHz frequency (16 kHz on our spectrograms due to an aliasing problem) are normally emitted by the NAA transmitter (44°38′N, 067°16′W). The signal between 1 and 3 kHz on the bottom spectrogram is a natural hiss band

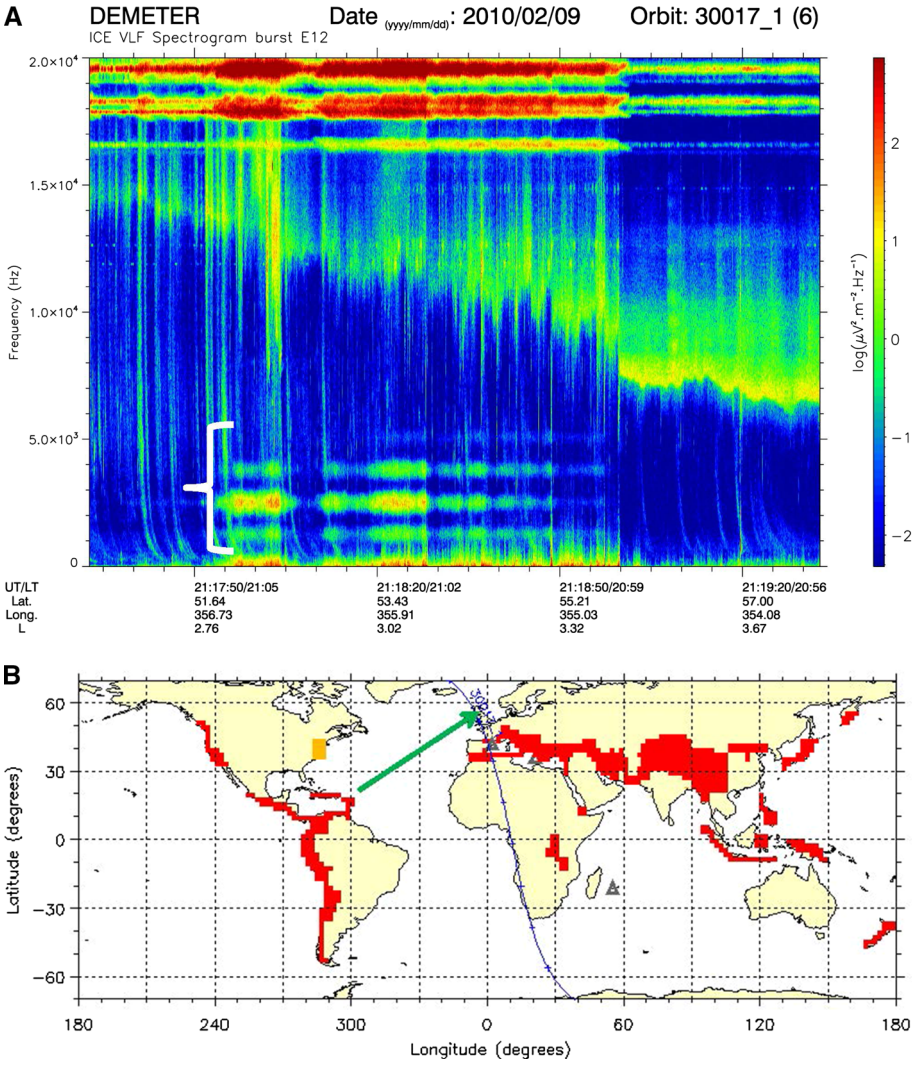

Fig. 3 Data recorded on February 9, 2010, between 21:17:30 and 21:19:30 UT. Up to 5 kHz, one can see lines (indicated by a *curly bracket*) due to the beating of frequencies from VLF transmitters. The panel below the spectrogram shows the half-orbit and the location of the event. The emission whose frequency decreases from 14.5 kHz at the beginning of the plot to 6.5 kHz at the end of the plot is related to the lower hybrid resonance (LHR) frequency. The sharp cutoff at 21:19:00 UT corresponds to the position of the trough in the ionosphere, i.e., to the position of the plasmapause at much higher altitudes

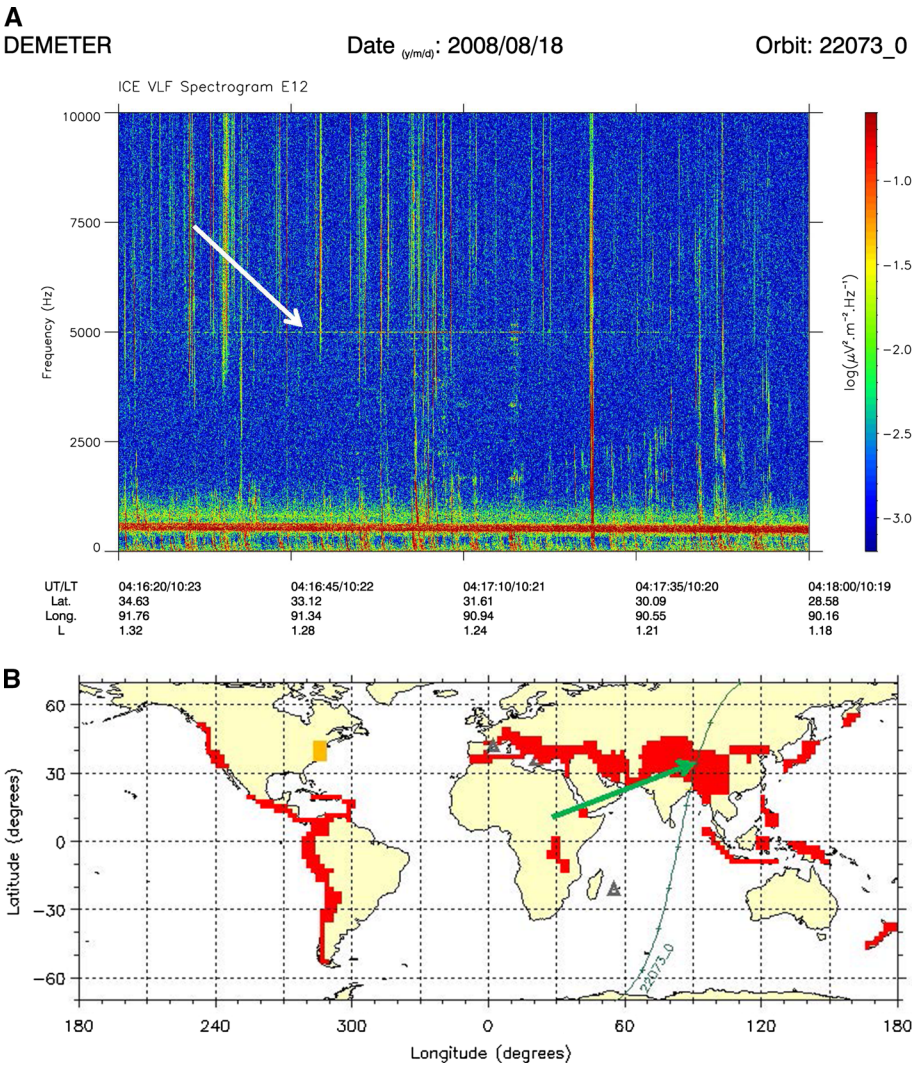

Fig. 4 VLF spectrogram of an electric field component recorded on August 18, 2008, between 04:16:20 and 04:18:00 UT in the frequency range 0–10 kHz. Pulses from an unlisted VLF transmitter are observed at 5 kHz (indicated by a *white arrow*). The natural emission around 450 Hz is limited by the local proton gyrofrequency. The panel below the spectrogram shows the half-orbit and the location of the event

separated by 360 Hz, and therefore, they are harmonics of the 60-Hz fundamental signal. Normally, the PLHR waves are observed between 1 and 4 kHz with a peak of occurrence around 2.5 kHz (Němec et al. 2007a). Nunn et al. (1999) explained that, in fact, these harmonic frequencies are emitted by industrial systems (see also Manninen 2005). The observation shown in Fig. 7 is unique; it is made above the USA (see the map below the spectrogram) where 60-Hz power lines are used. More precisely, the magnetically conjugate area of this event, just below the satellite, corresponds to the region of Seattle (3,500,000 inhabitants).

As opposed to PLHR, magnetospheric line radiation (MLR) appears as lines drifting in frequency and with a larger bandwidth. Although they have been extensively studied (Bell

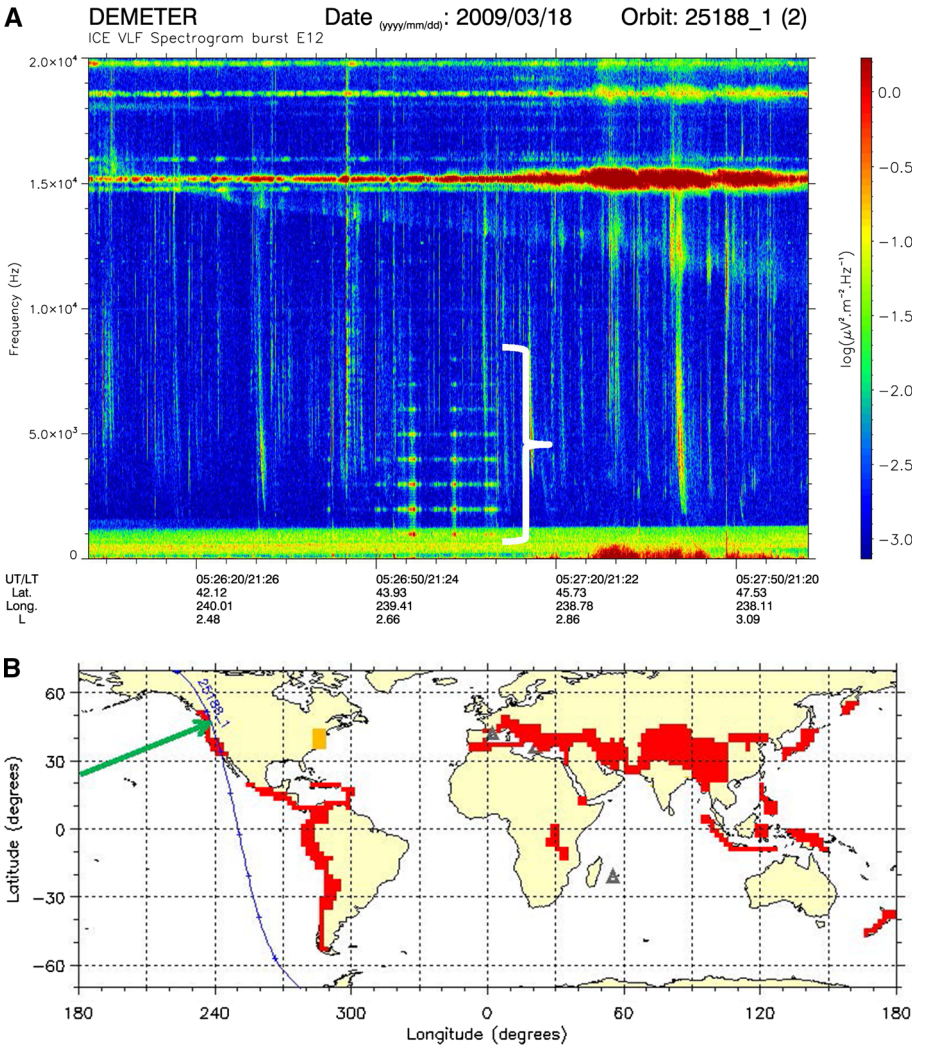

Fig. 5 Same as Fig. 1, but for data recorded on March 18, 2009, between 05:26:00 and 05:28:00 UT. A set of *lines* indicated by a *curly bracket* is observed up to 8 kHz in the vicinity of the NLK transmitter (48°12′N, 121°55′W). The *panel* below the spectrogram shows the half-orbit and the location of the event

et al. 1982; Rodger et al. 1995, 1999, 2000a, b; Manninen 2005; Parrot et al. 2007; Němec et al. 2007a, 2009a, b, 2012a, b), there is some controversy about the origin of these lines which are observed in space or on the ground because many of them are separated by neither 50 nor 60 Hz. An example of a spectacular MLR event is shown in Fig. 8 which displays 4 min of a VLF electric field spectrogram recorded on November 10, 2004 (the time of the largest magnetic storm during the DEMETER mission). Above 12 kHz, one can see another example of broadening of the α transmitter signals shown in Fig. 1. MLR waves are observed between 4 and 12 kHz. During this event, the MLR lines are particularly complex and they even show a time modulation.

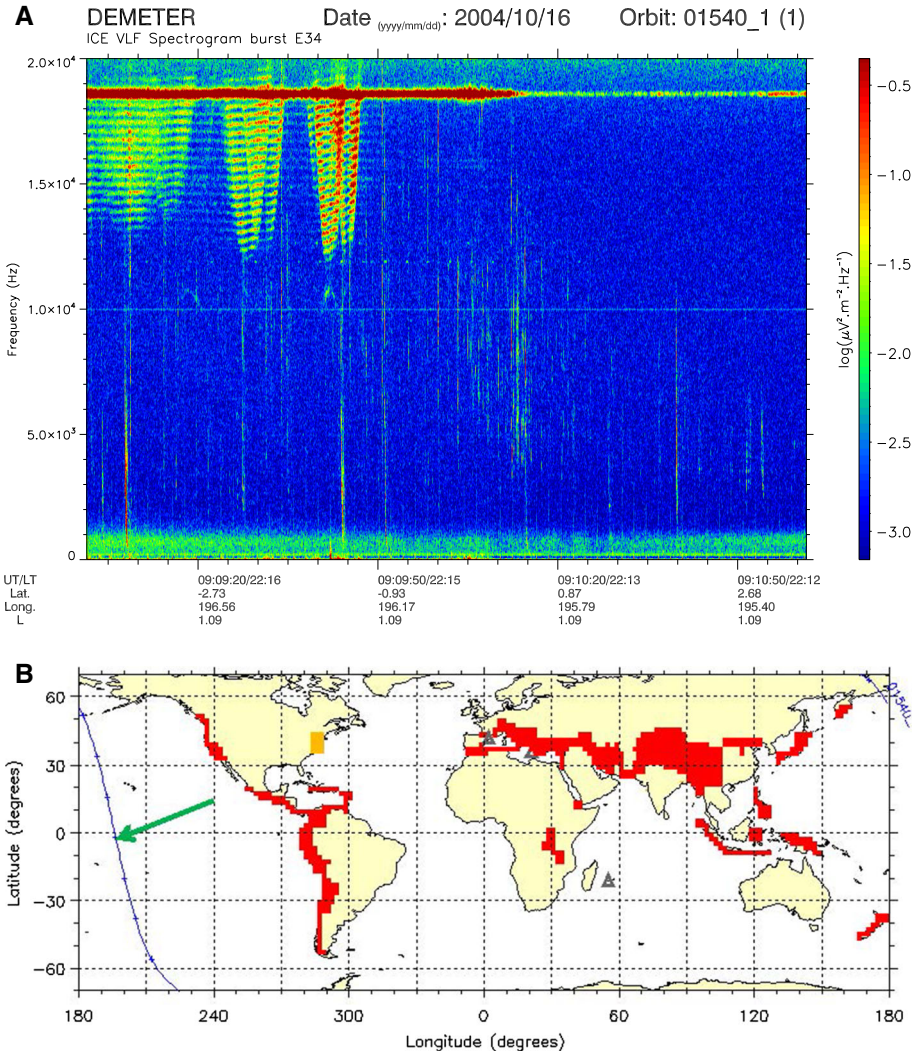

Fig. 6 VLF spectrogram of an electric field component recorded on October 16, 2004, between 09:09:00 and 09:11:00 UT in the frequency range 0–20 kHz. One can see unusual sidebands below the transmitter frequency. The *panel* below the spectrogram shows the half-orbit and the location of the event

4 QP Emissions

Although quasi-periodic (QP) emissions are very often observed by DEMETER in the ionosphere at least during sustained magnetic activity, only a few papers have been published up to now (Bespalov et al. 2010; Němec et al. 2013; Hayosh et al. 2013). A statistical analysis has been made by Hayosh et al. (2014). The characteristics of these QP emissions include a huge variety of locations, starting frequencies, frequency bands, slopes, and periodicities. One example is shown in Fig. 9 where data are recorded during three consecutive half-orbits on the nightside on November 9, 2006 (see the map). The top

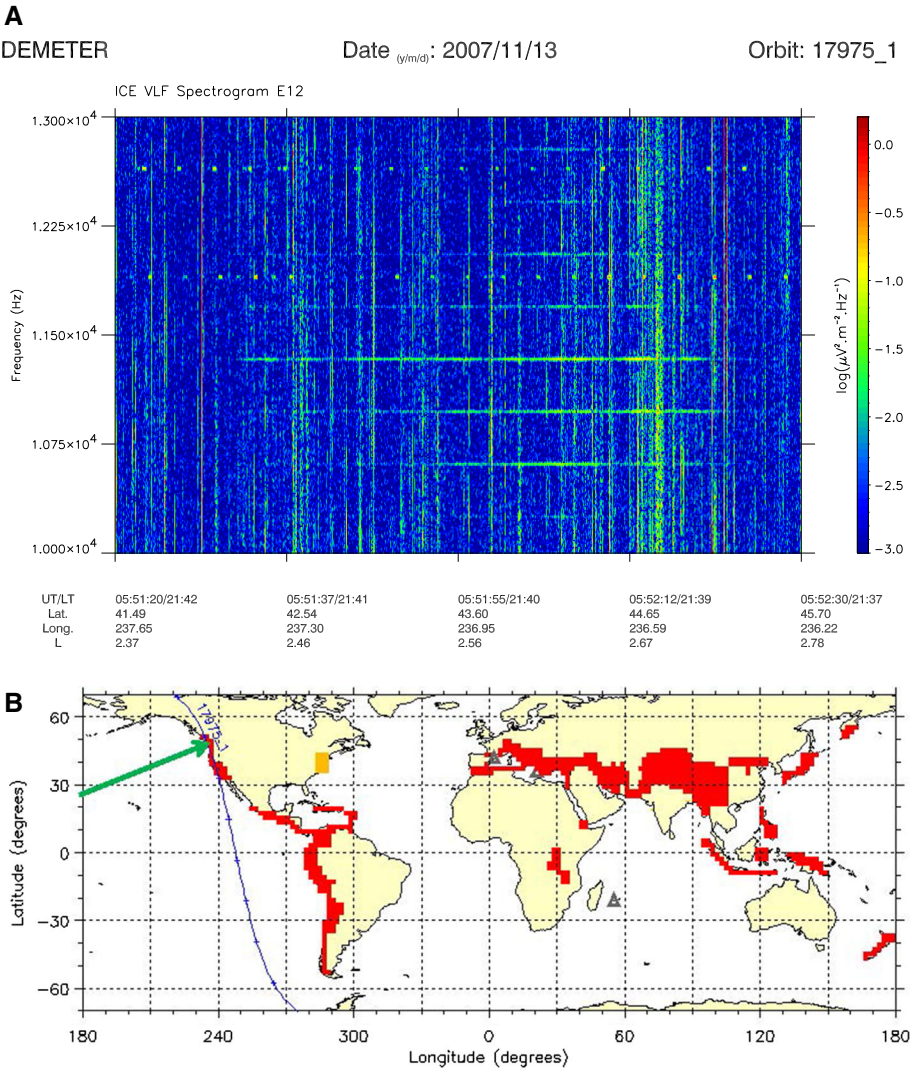

Fig. 7 VLF spectrogram of an electric field component recorded on November 13, 2007, between 04:16:20 and 04:18:00 UT in the frequency range 10–13 kHz. A set of *horizontal lines* is observed. The panel below the spectrogram shows the half-orbit and the location of the event

spectrogram shows a VLF electric field spectrogram between 0 and 3 kHz which is registered along a complete half-orbit during 36 min between 04:49:00 and 05:24:59 UT. One can see a set of QP emissions with a starting frequency around 1 kHz and with an average periodicity of the order of 6 min 10 s. These QP emissions are observed from the southern hemisphere (Lat = −72.88°) up to the northern hemisphere (Lat = 56.61°) including at the equator with a reduced intensity. The middle spectrogram concerns the next half-orbit where the data are recorded between 06:27:00 and 07:04:30 UT. The previous set of QP emissions is still present with a periodicity which is a little bit changed (5 min 50 s). Another set of QP emissions centered on 750 Hz appears with a lower frequency drift. In

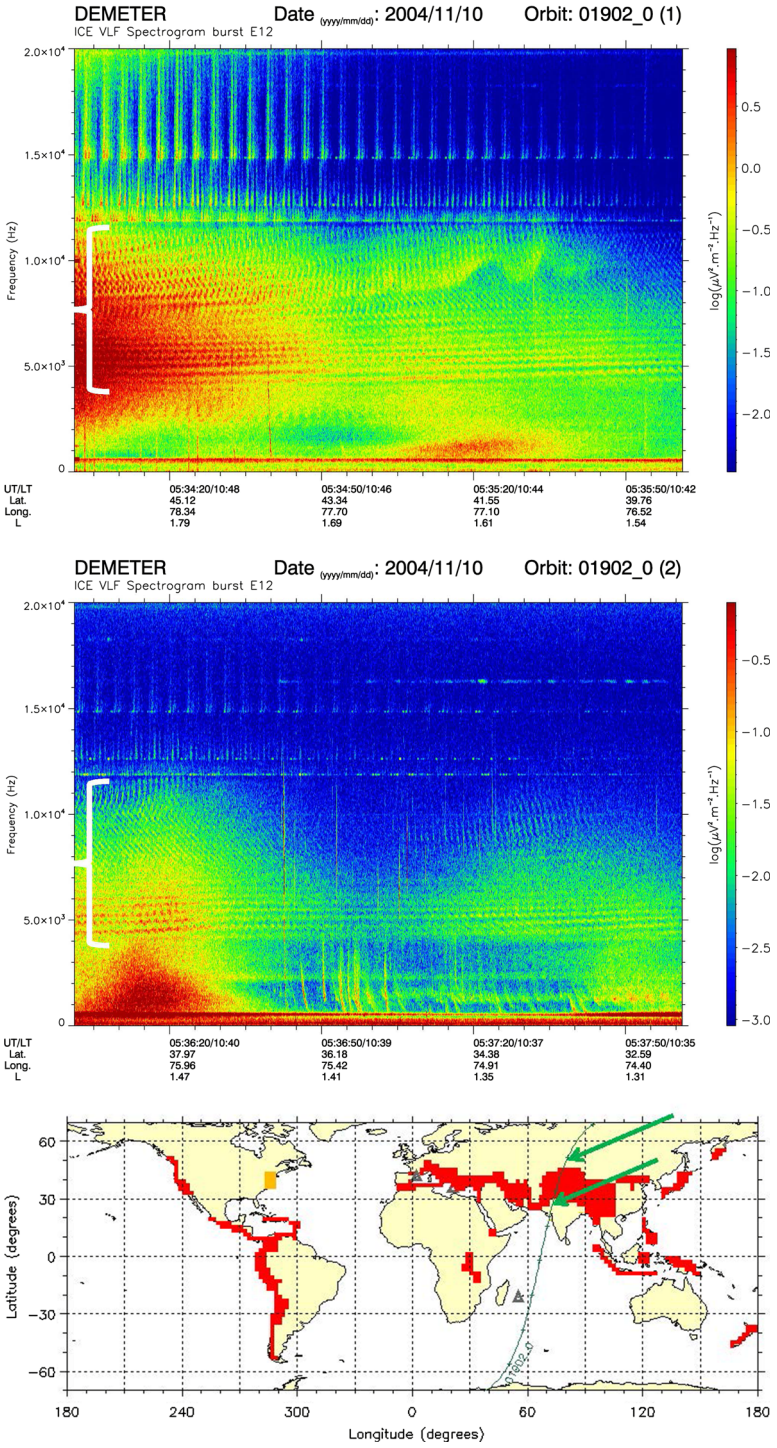
DEMETER Date (yyyy/mm/dd): 2004/11/10 Orbit: 01902_0 (1)
ICE VLF Spectrogram burst E12
Frequency (Hz)
log(μV².m⁻².Hz⁻¹)
UT/LT 05:34:20/10:48 05:34:50/10:46 05:35:20/10:44 05:35:50/10:42
Lat. 45.12 43.34 41.55 39.76
Long. 78.34 77.70 77.10 76.52
L 1.79 1.69 1.61 1.54
DEMETER Date (yyyy/mm/dd): 2004/11/10 Orbit: 01902_0 (2)
ICE VLF Spectrogram burst E12
Frequency (Hz)
log(μV².m⁻².Hz⁻¹)
UT/LT 05:36:20/10:40 05:36:50/10:39 05:37:20/10:37 05:37:50/10:35
Lat. 37.97 36.18 34.38 32.59
Long. 75.96 75.42 74.91 74.40
L 1.47 1.41 1.35 1.31
Latitude (degrees)
Longitude (degrees)

◀**Fig. 8** (*Top*) Spectrogram recorded on November 10, 2004, between 05:34:00 and 05:36:00 UT, (*middle*) continued until 05:38:00 UT. The two spectrogram panels show examples of MLR indicated by *curly brackets*. The emissions above 12 kHz are similar to those recorded in the top spectrogram of Fig. 1. Whistlers are observed after 05:36:40 UT in the bottom spectrogram and their *dispersion* indicates that they are coming from the southern hemisphere. The panel below the spectrograms shows the half-orbit and the location of the event is indicated by the two *green arrows*

the bottom spectrogram which corresponds to the next half-orbit and a time interval between 08:05:30 and 08:44:30 UT, the two sets of QP emissions are still present. This means that they cover a large part of the Earth in both hemispheres, including the equator ($\sim 50°$ in longitude at the equator), for at least 4 h on the nightside.

5 Equatorial Plasma Density During Magnetic Storms

DEMETER was mainly in operation during the declining phase of the unusually long solar cycle 23, but at the beginning in 2004 and 2005 several magnetic storms occurred. Due to the injection of ions into the ionosphere, it was the opportunity to record new ELF waves close to the ionospheric trough (Parrot et al. 2006, 2014b), and at mid-latitudes (Colpitts et al. 2012). It has also been shown that, in the equatorial region, there are plasma bubbles where lightning induces turbulence and ion heating occurs (Berthelier et al. 2008; Malingre et al. 2008; Pfaff et al. 2008). During these magnetic storms, many other plasma bubbles have been observed by DEMETER, and the largest one is presented in Fig. 10. It shows a very unusual variation of the plasma density during the magnetic storm of May 15, 2005, where the Dst index reaches a value of −247 nT at 09:00:00 UT (see the bottom panel). This time is close to the time of observation shown in Fig. 10. The electron density as well as the ion density presents a huge depletion by two orders of magnitude between 09:13:45 and 09:18:00 UT. This giant plasma bubble is located around the equator, and its latitudinal dimension is 1,830 km (see the map).

6 Whistlers and Related Phenomena

The waves propagating in the wave guide formed by the surface of the Earth and the bottom of the ionosphere are mainly due to thunderstorm activity (atmospherics). During the night, this waveguide has a cutoff frequency which is given by $f_n = n{\cdot}c/2\ h$, where c is the velocity of light, h the height of the ionosphere, and n the mode number. The first cutoff frequency ($n = 1$) is very often observed in fractional-hop (O^+) whistlers in the DEMETER VLF spectrograms and is of the order of 1.7 kHz on the nightside which corresponds to a height of the ionosphere equal to about 90 km. But this frequency may vary slightly; its detection on the VLF spectrograms has been used by Toledo-Redondo et al. (2012) to globally survey the height of the ionosphere around the Earth. On very rare occasions, several modes can be observed and one of these opportunities is shown in Fig. 11 which represents an electric field spectrogram recorded on July 14, 2010. The first order cutoff frequency is close to 1.7 kHz, and it can be seen that higher-order cutoff frequencies can be detected up to $n = 5$ (indicated by the white arrows).

Many sets of lines are also frequently observed in the nighttime. An example is given in the top spectrogram of Fig. 12 between 4 and 10 kHz (indicated by the curly brackets). These lines seem to be related to the thunderstorm activity, and more detailed explanations

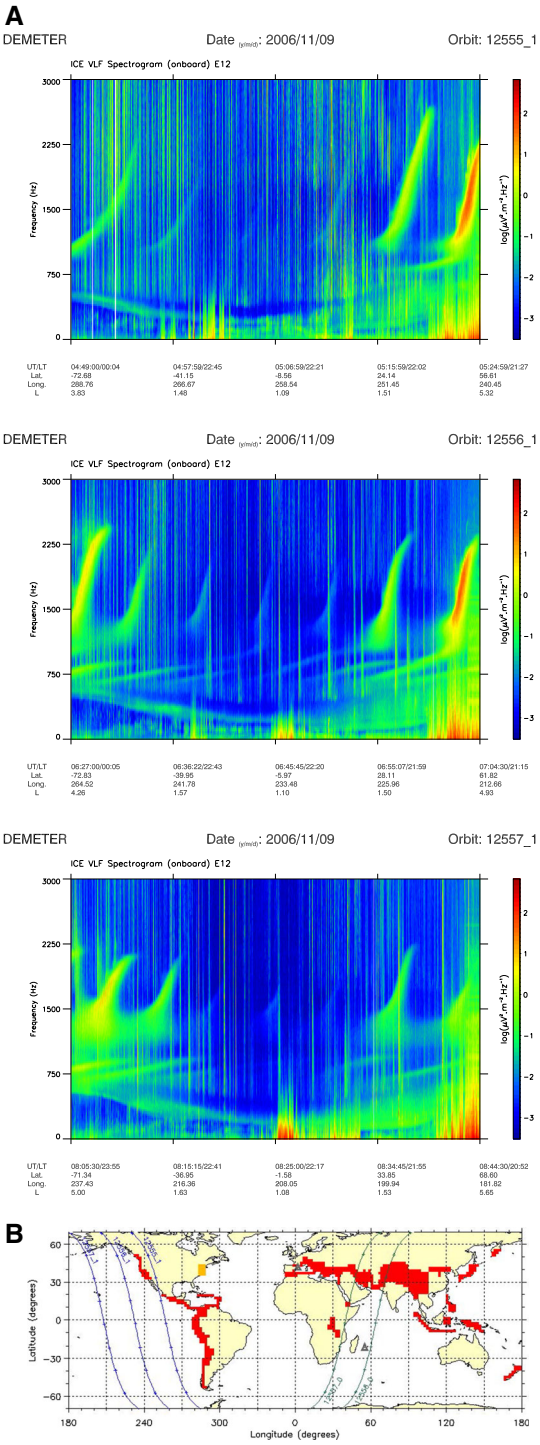

Fig. 9 First three panels are related to VLF electric field spectrograms between 0 and 3 kHz recorded during three consecutive half-orbits on November 9, 2006; (*top spectrogram*) between 04:49:00 and 05:24:59 UT, (*middle spectrogram*) between 06:27:00 and 07:04:30 UT, (*bottom spectrogram*) between 08:05:30 and 08:44:30 UT. The *three panels* display QP emissions. The *panel* below the spectrograms shows on the left the three corresponding up-going half-orbits (*blue color*)

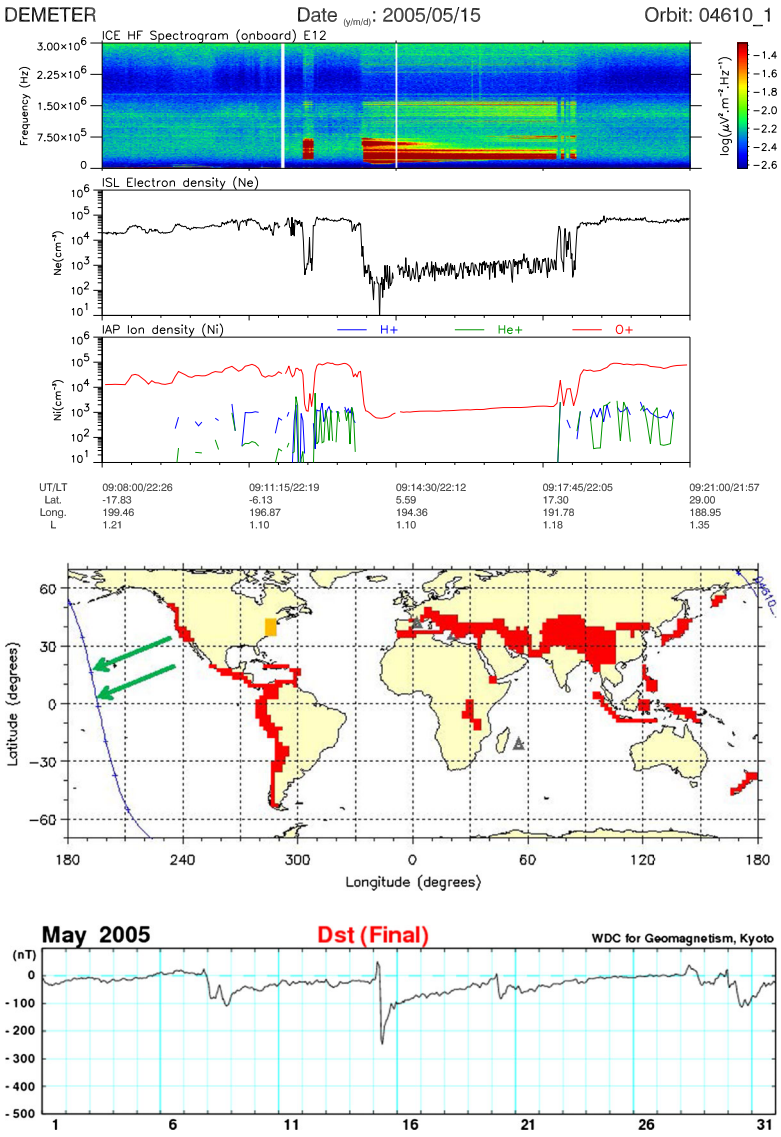

Fig. 10 First series of *three panels* is related to data recorded on May 15, 2005, between 09:08:00 and 09:21:00 UT. From the top to the bottom, the *first panel* shows the HF electric field spectrogram up to 3 MHz, the electron density is plotted in the *second panel* and the ion density is shown in the *third panel*; this shows an equatorial plasma bubble. Then, the *fourth panel* shows the half-orbit and the location of the event is indicated by the two *green arrows*. The *last panel* displays the Dst variation during May 2005, from the World Data Center (WDC) for Geomagnetism in Kyoto

will be given in a forthcoming paper. It must be noticed that these lines are very different from the V-shaped emissions observed above powerful thunderstorms (Parrot et al. 2008a; El-Lemdani Mazouz et al. 2011).

It has been shown by Fiser et al. (2010) that the whistler intensities recorded onboard DEMETER depend on the intensities of the lightning strokes and on their distance to the satellite. An interesting feature concerning the intensities of strong whistlers recorded by DEMETER is shown in Fig. 12. The top spectrogram concerns a VLF electric field spectrogram recorded on February 27, 2007, between 05:57:00 and 05:59:00 UT. One can see at 05:58:22 UT (indicated by a white arrow) a very intense whistler without noticeable dispersion (see also the second spectrogram), which is very different from the usual dispersion of 0^+ whistlers observed by DEMETER [Santolik et al. 2008, 2009]. The origin of this whistler is due to a powerful positive cloud-to-ground (+CG) lightning stroke with a very large peak current of 180 kA which occurred above the Pacific ocean, approximately 80 km

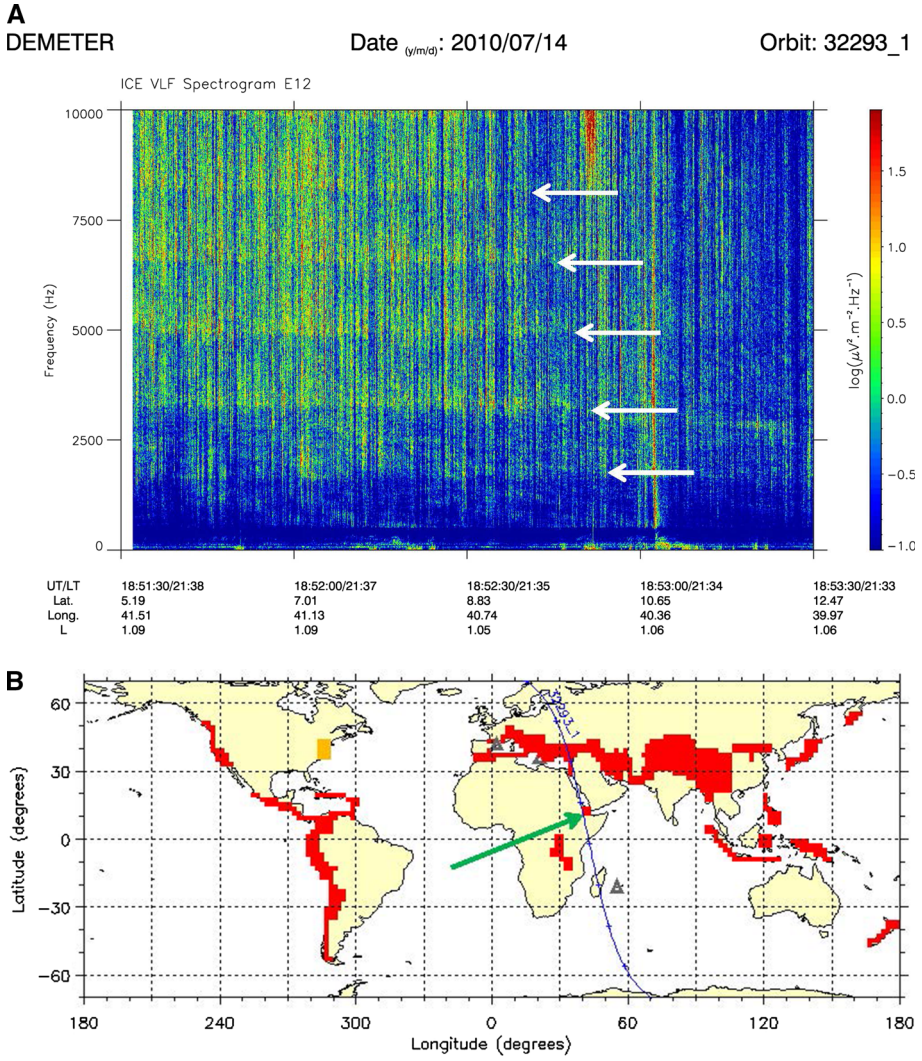

Fig. 11 Data recorded on July 14, 2010, between 18:51:30 and 18:53:30 UT. Several cutoff frequencies of the waves propagating in the Earth-ionosphere waveguide can be observed (see text). The panel below the *spectrogram* shows the half-orbit and the location of the event

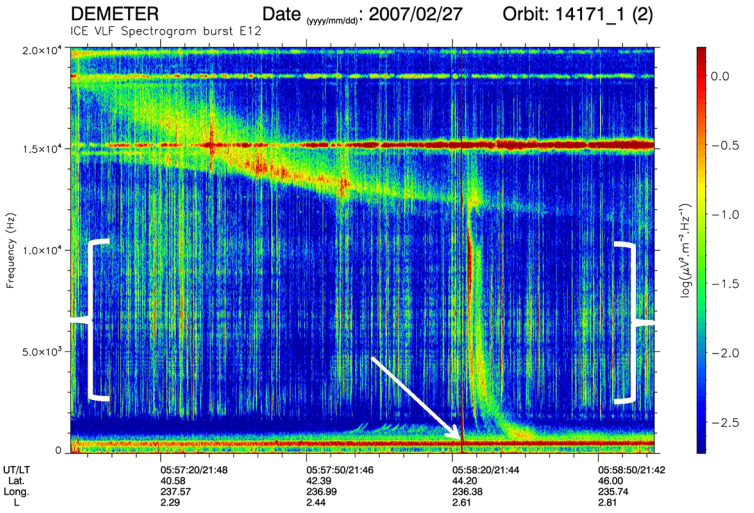
DEMETER
Date (yyyy/mm/dd): 2007/02/27
Orbit: 14171_1 (2)
ICE VLF Spectrogram burst E12
Frequency (Hz)
log(μV².m⁻².Hz⁻¹)
UT/LT
Lat.
Long.
L
05:57:20/21:48
40.58
237.57
2.29
05:57:50/21:46
42.39
236.99
2.44
05:58:20/21:44
44.20
236.38
2.61
05:58:50/21:42
46.00
235.74
2.81

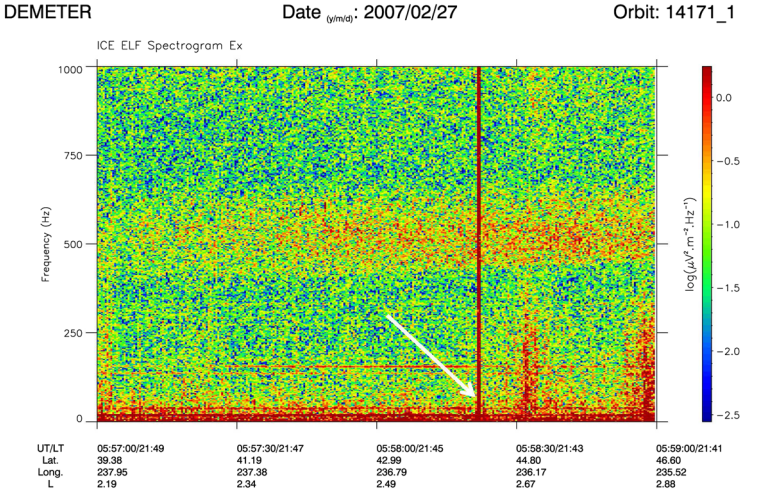
DEMETER
Date (y/m/d): 2007/02/27
Orbit: 14171_1
ICE ELF Spectrogram Ex
Frequency (Hz)
log(μV².m⁻².Hz⁻¹)
UT/LT
Lat.
Long.
L
05:57:00/21:49
39.38
237.95
2.19
05:57:30/21:47
41.19
237.38
2.34
05:58:00/21:45
42.99
236.79
2.49
05:58:30/21:43
44.80
236.17
2.67
05:59:00/21:41
46.60
235.52
2.88

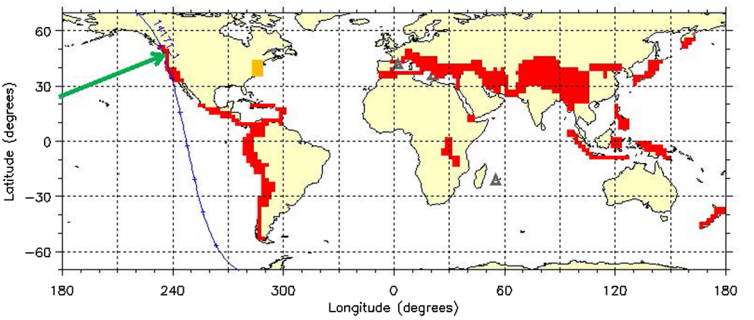
Latitude (degrees)
Longitude (degrees)

◀**Fig. 12** (*Top spectrogram*) Data recorded on February 27, 2007, between 05:57:00 and 05:59:00 UT (data in the VLF range); (*bottom spectrogram*) frequency zoom (0–1 kHz) of the top spectrogram (data in the ELF range). The two *spectrograms* show a whistler indicated by a *white arrow* without noticeable dispersion. In the top spectrogram two *curly brackets* indicate a set of lines (see text). The *panel* below the spectrograms shows the half-orbit and the location of the event

west of the coast and 180 km northwest of the vertical footprint of DEMETER (national lightning detection network—NLDN data, courtesy of Ryan Said, Stanford University). Other very intense lightning strokes occurred before the arrival of the satellite in the same area. This event is not unique and many other whistlers without noticeable dispersion can be observed in the DEMETER data. The whistlers always originate from strong lightning strokes occurring just below the satellite. It was suspected that this intense whistler signal can produce saturation inside the electronics of the experiment, but the ELF and VLF waveforms do not show saturation. A Fourier analysis with large time resolution shows that, in fact, this whistler at low frequencies has two branches: one with a small dispersion and another without dispersion. The debate is not closed, and a paper with much more detailed explanations is in preparation.

In the top spectrogram of Fig. 12, one can see a wedge-like shape formed by whistlers at the beginning of the plot between 13 and 19 kHz (see also another example in the right spectrogram of Fig. 1). The lower- and upper-frequency cutoffs of this wedge-like form have been explained by Shklyar et al. (2010) in terms of wave propagation. An important point is that, at its altitude, the satellite is in a trough of the height profile of the lower hybrid resonance (LHR) frequency and then the maximum of the LHR frequency is above the satellite. The waves with frequencies below the LHR maximum are reflected above the satellite, which explains the lower cutoff frequency. The upper cutoff frequency is due to another feature of unducted VLF wave propagation.

7 SETI Events

This section is related to the most astonishing phenomena ever recorded by DEMETER. On the nighttime part of the orbit, very spectacular events called structured emissions with turbulence and interference (SETI) by the PI of the experiment are observed as illustrated by Fig. 13 which represents a VLF electric field spectrogram recorded on April 24, 2007 (other events can be seen in Píša 2012). An intense and unstructured VLF turbulence event is observed up to ~ 2 kHz at the central location which appears to trigger structured narrow band harmonic emissions observed on either side of the central location and characterized by a few hundred Hz frequency variation of the fundamental over a few tens of seconds. The turbulence observed in the middle of the event lasts 30–50 s along the orbit, but the structured harmonic emissions may be detected during 1 min, or more, both before and after. The plasma measurements of electron density and temperature Ne and Te do not show any anomalous conditions that may induce a drastic change in the coupling between the ICE instrument and the plasma, and thus in the actual operation of the ICE probes, which may be responsible for anomalous signals such as those observed. The 1-Hz modulation of the VLF signal intensity must be generated by some interference between the ISL Langmuir probe (Lebreton et al. 2006) sweeps (from -3 to $+3$ V in relation to satellite ground potential) and the ICE probes and remains, as well, totally unexplained. The 1-s periodicity is associated with the sweep of the ISL Langmuir probe. When the probe collects the highest electron current, the spacecraft (S/C) floating potential becomes

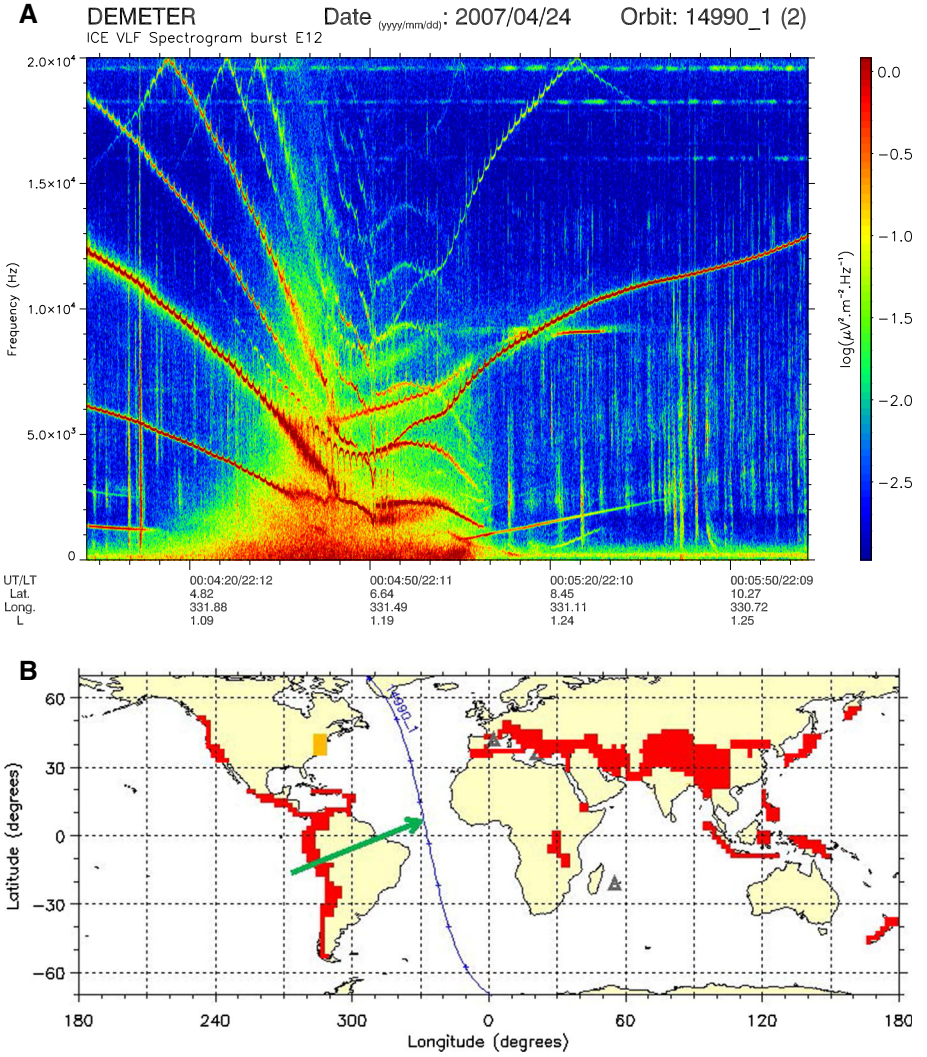

Fig. 13 Spectrogram recorded on April 24, 2007, between 00:04:00 and 00:06:00 UT. In the top of the spectrogram, the filamentary structures seem to be reflected at 20 kHz due to spectrum aliasing (see text for explanation). The *panel* below the spectrogram shows the half-orbit and the location of the event

slightly more negative by less than ∼20 mV, but there is no reason for the S/C potential to have any effect on the waves detected by ICE. One may suggest that instabilities of the ISL sheath may beat with the VLF waves to produce frequency variations, but this is purely speculative and one must admit that, at the moment, no explanation can be seriously proposed. SETI events recorded when ISL was *OFF* do show the VLF harmonic emissions, of course without the 1-Hz modulation. This rules out the existence of an unknown mechanism associated with ISL that may trigger the VLF emissions.

Many SETI events have been recorded at least at the beginning of the mission because the occurrence of these phenomena dramatically decreased after 2006. This might indicate

a relationship between the SETI events and either the average ionospheric conditions, because of the decreasing solar flux after 2006, or the average magnetospheric activity since the occurrence of disturbed conditions also decreased significantly in the same period according to magnetic activity indices. A global map of the detected SETI events is given in Fig. 14 showing that they occur close to the magnetic equator, over South America and, to a lesser extent, over Africa and the Indian Ocean, but predominantly in the region of the South Atlantic Geomagnetic Anomaly (SAGA) over South America and the Atlantic Ocean. One may note that the region of maximum occurrence over the Atlantic also lies in the Intertropical Convergence Zone (ITCZ) which, curiously, is nearly parallel to the magnetic equator. Erratic weather patterns with stagnant calms and violent thunderstorms common to the ITCZ might be suspected of generating sporadically very intense EM emissions. However, some SETI events also occur along the magnetic equator in the Indian Ocean while, there, the two branches of the ITCZ are clearly displaced $\sim 10°$–$5°$ to north and south, which seems to rule out the ITCZ hypothesis. Figure 15 shows the monthly relative occurrence of SETI events during the period between August 2004 and July 2006, with a maximum in June.

Finally, one may look for phenomena that develop in disturbed plasma conditions not seen by DEMETER because they occur at lower altitudes, below the DEMETER orbit. Equatorial plasma bubbles (EPBs) do, of course, appear as good candidates and we have searched among recently published observations to see whether there is any evidence of similar seasonal and geographic statistical variations. EPBs have been detected by numerous satellites such as DMSP, ROCSAT, COSMIC, CHAMP, GRACE, and CNOF/S, but only CHAMP, GRACE, and CNOF/S performed measurements at low enough altitudes. A solar cycle dependence with a maximum at high solar activity was indeed observed by Huang et al. (2014), but over the whole range of altitudes of CNOF/S (up to 850 km). Yizengaw et al. (2013) showed a maximum of occurrence in June, but at altitudes

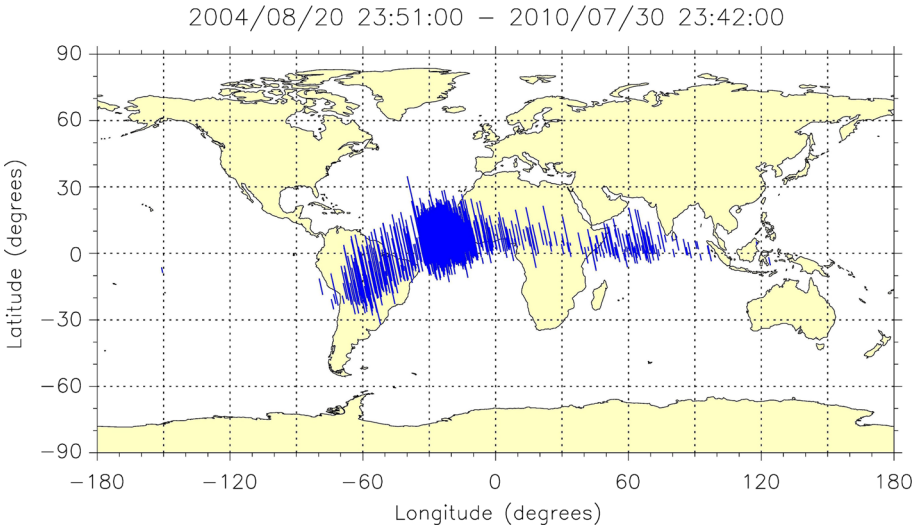

Fig. 14 Map showing the location of events similar to the one reported in Fig. 13. All events between August 20, 2004, and July 30, 2010, are considered. The *blue lines* represent the part of the orbits where the events are observed

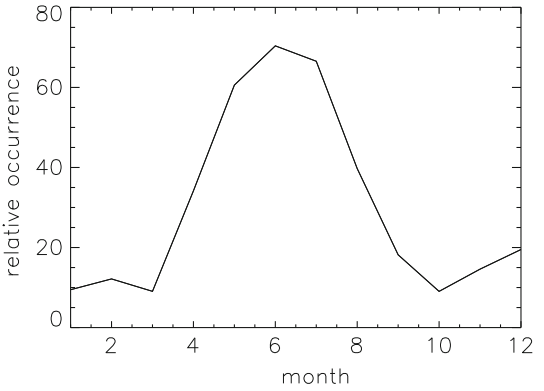

Fig. 15 Histogram of events similar to the one reported in Fig. 13 as function of the months between August 2004 and July 2006. The values are normalized by the total number of events

larger than 500 km, thus encompassing the DEMETER orbit and not satisfying the altitude criterion indicated above and, in addition, corresponding to the late night LT sector 00–06 and thus very different from the ~21–23 LT sector of DEMETER which lies closer to sunset and to the major LT sector of EPB occurrence of 19–22. Dao et al. (2011) found a June–July–August maximum, but they consider the whole night sector 18–06 LT and the whole range of CNOF/S altitudes which does not satisfy the low altitude only criterion and cannot be used as a strong argument. On the contrary, at least three arguments may be raised against a possible idea that EPBs at low altitude produce SETI events observed at DEMETER:

1. due to the extension of the EPB plasma depletion along the Earth's magnetic field, some plasma depletion should also be observed for most cases by DEMETER when crossing the corresponding tube of force, which is not the case,
2. since EPBs on DEMETER never trigger SETI events, there is no reason for EPB at slightly lower altitudes (~400–450 km) to trigger such events, and
3. if DEMETER only detects emissions produced at some distance, there is no reason for the ISL 1-Hz modulation to be superimposed, since such a modulation is never seen among the many cases when high-intensity natural VLF waves are detected (whistlers, auroral emissions, etc.).

Altogether, the idea that SETI may result from phenomena at some distance below DEMETER cannot be supported by DEMETER and other satellite data.

Another curious behavior of the ICE experiment is shown in Fig. 16 where data recorded on March 22, 2006, between 06:10:00 and 06:12:00 UT are presented. It can be seen that the lower hybrid resonance (LHR) frequency, which decreases from 14 kHz at the beginning of the plot to 9 kHz at the end of the plot, is surrounded by filamentary electrostatic noise (indicated by a white arrow in the figure). This noise follows the decrease in the LHR and has a frequency bandwidth of the order of 5 kHz. There are other similar events, but they are not so numerous as the SETI events and no particular location has been found for their occurrence. Because electrostatic emissions around the LHR are concerned, we can establish a parallel between these events and the one published by Parrot et al. (2008b) where the plasma conditions were particular due to ion injection into the ionosphere during the recovery phase of a small magnetic storm. On March 22, 2006, the magnetic activity was also non negligible.

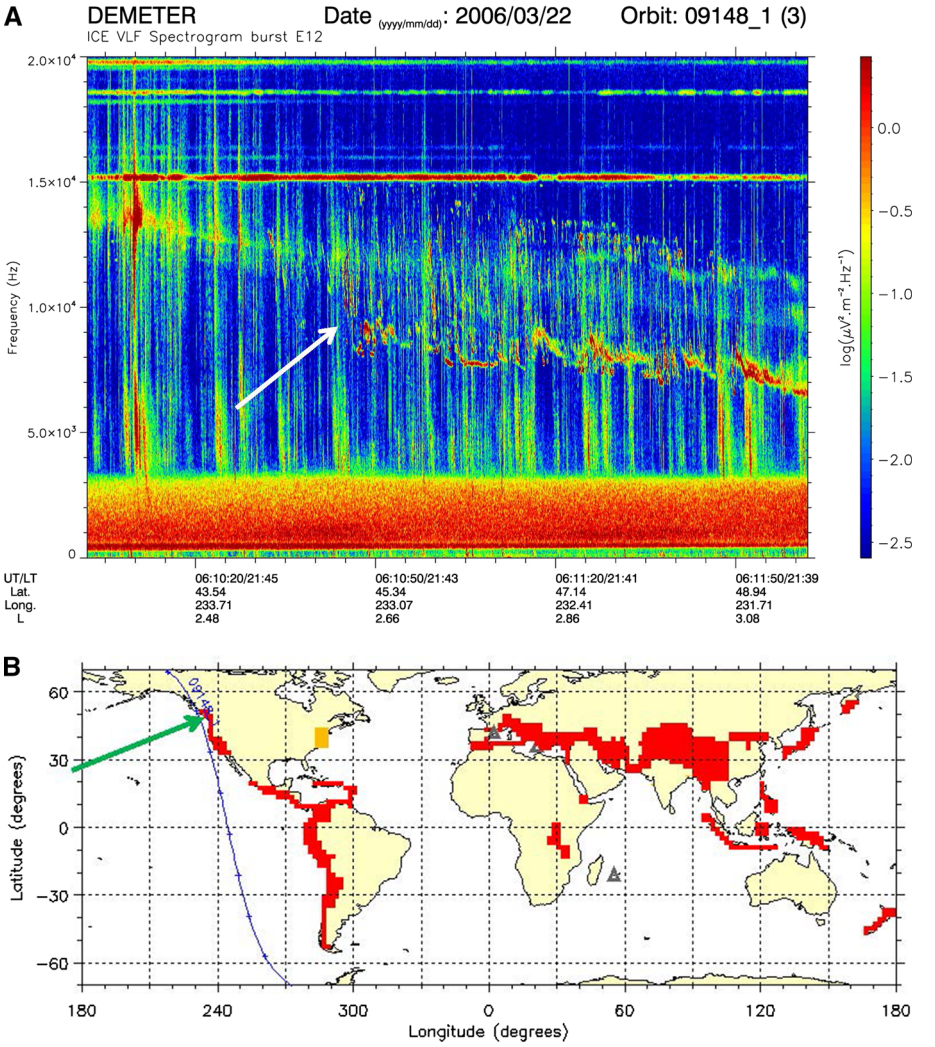

Fig. 16 Spectrogram recorded on March 22, 2006, between 06:10:00 and 06:12:00 UT. A noise is observed around the decreasing LHR frequency (see text). The *panel* below the spectrogram shows the half-orbit and the location of the event

8 Pacific Equatorial Anomaly

In the close vicinity of the dip equator in the Pacific sector (between $-2°$ and $+2°$ geomagnetic latitude), two surges of electrostatic turbulence are often observed on the electric field along the S_1S_2 axis, which is horizontal and perpendicular to the orbit trajectory (Fig. 17a): first, a narrow band of electrostatic turbulence with a frequency decreasing from $\sim$600 to $\sim$200 Hz ending with an unstructured enhancement down to a few Hz, then a sharp peak of electrostatic turbulence from a few Hz to $\sim$600–800 Hz. The dip equator is located between these two electrostatic emissions, and the second signal is often

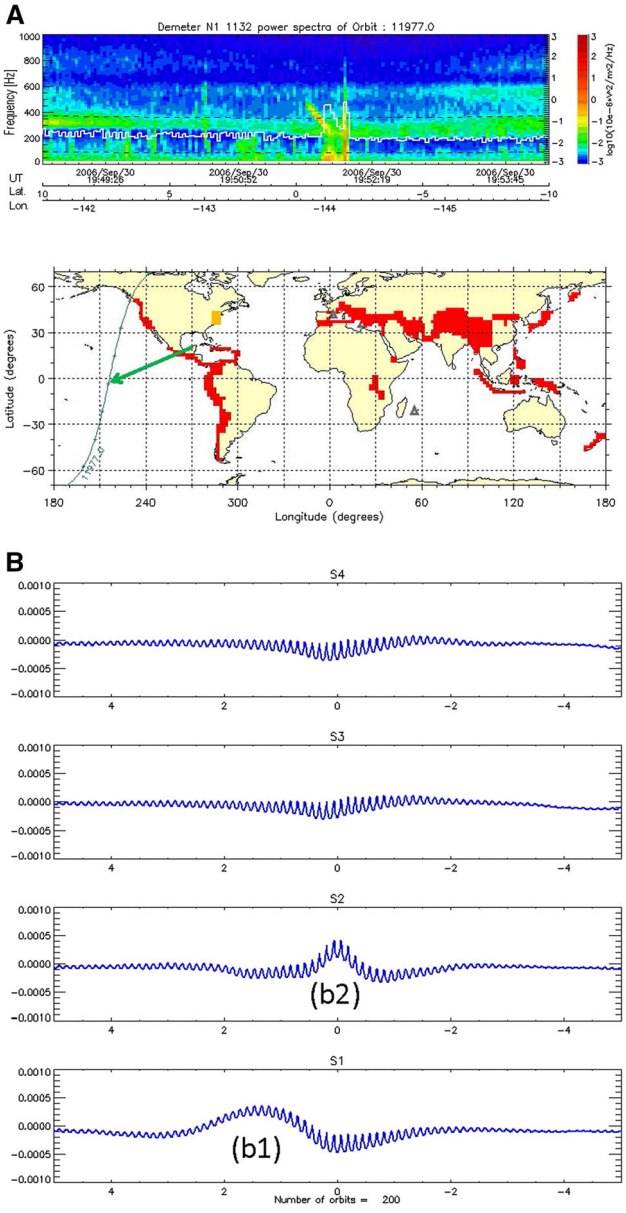

Fig. 17 **a** ICE VLF spectrogram (Orbit 11977.0), with UT, geocentric latitude and longitude along the *X-axis* and the superimposed *white line* displaying the power spectral density at 20 Hz (scale indicated on the *Y-axis* on the right). **b** Detrended potentials in volts of the four ICE probes S_1, S_2, S_3, and S_4 averaged over 200 crossings of the dip equator in the Pacific sector. The geomagnetic latitude is indicated on the *X-axis*; the geomagnetic equator does not exactly coincide with the dip equator defined as the location where the vertical component of the Earth magnetic field is zero. The increase in the S_1 and S_2 potentials are associated with the first broader and the second sharper peak of electrostatic turbulence observed on the VLF spectrograms. The superimposed fast modulations result from the S/C floating potential variation due to the ISL Langmuir probe sweeps. (*b1*) and (*b2*) are potential disturbances explained in the main text. The *panel* below the VLF spectrogram in **a** shows the half-orbit and the location of the event

more visible and intense than the first. Simultaneous with these two surges, the ICE probes record slight but systematic variations of potential measured with respect to the S/C. The potential variation can be associated with the S/C floating potential variation as the probes are maintained at a constant potential with respect to the plasma. In this case, all four probes should show overall potential increases simultaneously, which is not the case here. A comparison of detrended potential variations of the four probes averaged over 200 orbits (Fig. 17b) shows potential increases with the first maximum of $\sim$3–4 mV on the S_1 potential at $\sim$1.5° north (represented by b1) and the second maximum of $\sim$3 mV close to 0° on the S_2 probe potential (represented by b2). Apart from the S/C floating potential decrease, a probe potential may be increased independently of other probes in order to counteract a decrease in the electron current collection by the probe. The mechanism of the electron current decrease is still unknown.

These events are observed only on dayside suborbits in the Pacific sector. The condition for this anomaly to occur is that the angle between the local magnetic field and the satellite velocity is less than $\sim$2.5°. In the Pacific sector (longitude between 160°W and 120°W), the dip equator inclined along a $\sim$ northwest–southeast direction and the orbit inclination combine to satisfy this condition on dayside satellite passes. A tentative interpretation relies on the dependence of the S/C–plasma interaction and the formation of the wake at an angle between the Earth's magnetic field and the satellite velocity. Rehman et al. (2013) performed a kinetic simulation of a S/C–plasma interaction when the S/C velocity is nearly aligned with the local geomagnetic field and found small but distinct variations of the S/C floating potential that explains part of the DEMETER data. This configuration requires a 3-D numerical domain of the wake region to be expanded at least 30 m behind the satellite. However, due to the smallness of the signal and inherent statistical noise, the comparison with DEMETER data did not provide unambiguous conclusions and, in particular, the occurrence of distinct electrostatic emissions is not understood yet.

9 Interference

Electromagnetic compatibility (EMC) problems have been taken into account since the beginning of the project and special requirements have been considered for some platform devices (Cussac et al. 2006). But despite careful tests during the integration of the experiments on the satellite platform before the launch, there still exists interference in the wave experiment data which have been observed in space. They are described by Lagoutte et al. (2005). They are at a low enough level not to prevent the scientific use of the data except in two cases:

- The magnetic field experiment is perturbed in the frequency range 1–8 kHz,
- The electric field experiment is perturbed in the complete HF range during daytime (problem due to the solar panel).

These interference signals normally appear as lines at constant frequencies in a spectrogram but, during the mission, a very unusual interference has been discovered in the high-resolution data (see Fig. 18 between 06:27:57 and 06:28:07 UT). Its duration is of the order of 10 s and the emission covers the complete VLF range. It has not been possible to determine the origin of this signal because it is not periodic. Fortunately, it does not occur often. The emissions observed in the top right corner of Fig. 18 are parts of VLF saucers (see James et al. 2012).

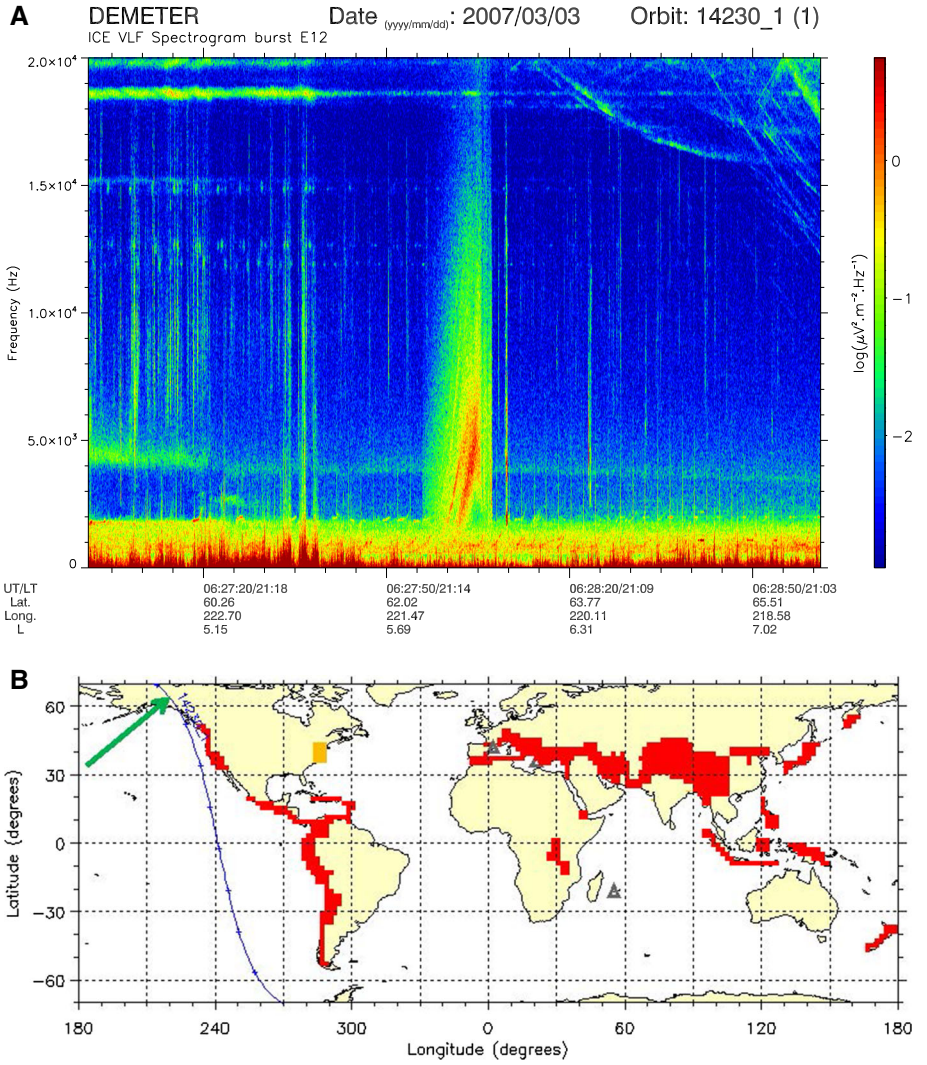

Fig. 18 Data recorded on March 03, 2007, between 06:27:00 and 06:29:00 UT. One can see interference produced onboard the satellite. The *panel* below the spectrogram shows the half-orbit and the location of the event

To maintain the satellite attitude, magnetotorquers have been used (Cussac et al. 2006), and this induces interference on the magnetic field components and, to a small extent, on the ULF range of the electric components (Lagoutte et al. 2005). These interference signals can be easily detected on the quick-look plots (Lagoutte et al. 2006); they occur at latitudes around −45°, 0°, and +45° during the beginning of the mission until October 13, 2004 (from half-orbit 00001.0 to half-orbit 01497.0). After this date, the magnetotorquers have only been activated when the invariant latitude of the orbit is larger than 65°. Then, these interference events are also observed when data have been recorded beyond this limit (see Sect. 1).

10 Conclusions

During its more than 6 years in the Earth's ionosphere, DEMETER has witnessed a great diversity of various phenomena. Up to now, more than 260 scientific papers have been published with the DEMETER data. They are listed on http://smsc.cnes.fr/DEMETER/A_publications.htm. Some other registered phenomena are very unusual. They include known events with large intensities, unknown man-made radio emissions, and unexpected plasma conditions which lead to electronic problems. The aim of this paper was to keep track of these events for scientists using the DEMETER data or for those involved in future LEO missions to be launched in 2016 such as TARANIS (Lefeuvre et al. 2008) or CSES (Shen et al. 2011). At this time, studies concerning some events are still on-going. These concern MLR emissions, QP emissions (including comparison with ground-based stations), whistlers without dispersion, sets of lines associated with whistlers as shown in the top of Fig. 12, and SETI events.

Acknowledgments DEMETER was a CNES mission. We thank the engineers from CNES and scientific laboratories (CBK, IRAP, LPC2E, LPP, SSD of ESTEC) who largely contributed to the success of this mission. Thanks are also due to many students who carefully scrutinized the DEMETER data during their summer jobs. OS and DP acknowledge funding from projects M100421206, GACR14-31899S, and LH12231. FN was supported by GACR Grant P209/12/P658. The work of TO was supported through the IODISSEE ANR grant.

References

Bell TF (1985) High-amplitude VLF transmitter signals and associated sidebands observed near the magnetic equatorial plane on the ISEE 1 satellite. J Geophys Res 90(A3):2792–2806

Bell TF, Inan US, Helliwell RA (1981) Nonducted coherent VLF waves and associated triggered emissions observed on the ISEE-1 satellite. J Geophys Res 86(A6):4649–4670

Bell TF, Luette JP, Inan US (1982) ISEE 1 observations of VLF line radiation in the Earth's magnetosphere. J Geophys Res 87(A5):3530–3536

Bell TF, Inan US, Piddyachiy D, Kulkarni P, Parrot M (2008) Effects of plasma density irregularities on the pitch angle scattering of radiation belt electrons by signals from ground based VLF transmitters. Geophys Res Lett 35:L19103. doi:10.1029/2008GL034834

Bell TF, Graf K, Inan US, Piddyachiy D, Parrot M (2011) DEMETER observations of ionospheric heating by powerful VLF transmitters. Geophys Res Lett 38:L11103. doi:10.1029/2011GL047503

Berthelier JJ, Malingre M, Pfaff R, Seran E, Pottelette R, Jasperse J, Lebreton JP, Parrot M (2008) Lightning-induced plasma turbulence and ion heating in equatorial ionospheric depletions. Nat Geosci 1:101–105. doi:10.1038/ngeo109

Bespalov PA, Parrot M, Manninen J (2010) Short-period VLF emissions as solitary envelope waves in a magnetospheric plasma maser. J Atmos Sol Terr Phys 72:1275–1281

Clilverd MA, Rodger CJ, Gamble R, Meredith NP, Parrot M, Berthelier JJ, Thomson NR (2008) Ground-based transmitter signals observed from space: ducted or nonducted? J Geophys Res 113:A04211. doi:10.1029/2007JA012602

Colpitts CA, Cattell CA, Kozyra JU, Parrot M (2012) Satellite observations of banded VLF emissions in conjunction with energy-banded ions during very large geomagnetic storms. J Geophys Res 117:A10211. doi:10.1029/2011JA017329

Cussac T, Clair MA, Ultré-Guerard P, Buisson F, Lassalle-Balier G, Ledu M, Elisabelar C, Passot X, Rey N (2006) The DEMETER microsatellite and ground segment. Planet Space Sci 54:413–427. doi:10.1016/j.pss.2005.10.013

Dao E, Kelley MC, Roddy P, Retterer J, Ballenthin JO, de La Beaujardiere O, Su YJ (2011) Longitudinal and seasonal dependence of nighttime equatorial plasma density irregularities during solar minimum detected on the C/NOFS satellite. Geophys Res Lett 38:L10104. doi:10.1029/2011GL047046

El-Lemdani Mazouz F, Pinçon JL, Parrot M, de Feraudy H, Lehtinen NG, Lefeuvre F (2011) Asymmetric V-shaped streaks recorded on board DEMETER satellite above powerful thunderstorms. J Geophys Res 116:A11321. doi:10.1029/2011JA016794

Fiser J, Chum J, Diendorfer G, Parrot M, Santolik O (2010) Whistler intensities above thunderstorms. Ann Geophys 28:37–46

Gamble RJ, Rodger CJ, Clilverd MA, Sauvaud JA, Thomson NR, Stewart SL, McCormick RJ, Parrot M, Berthelier JJ (2008) Radiation belt electron precipitation by man-made VLF transmissions. J Geophys Res 113:A10211. doi:10.1029/2008JA013369

Hayosh M, Pasmanik DL, Demekhov AG, Santolik O, Parrot M, Titova EE (2013) Simultaneous observations of quasi-periodic ELF/VLF wave emissions and electron precipitation by DEMETER satellite: a case study. J Geophys Res Space Phys. doi:10.1002/jgra.50179

Hayosh M, Němec F, Santolík O, Parrot M (2014) Statistical investigation of VLF quasi-periodic emissions measured by the DEMETER spacecraft. J Geophys Res Space Phys 119:8063–8072. doi:10.1002/2013JA019731

Helliwell RA, Katsufrakis JP, Bell TF, Raghuram R (1975) VLF line radiation in the Earth's magnetosphere and its association with power system radiation. J Geophys Res 80(31):4249–4258

Huang C-S, de La Beaujardiere O, Roddy PA, Hunton DE, Liu JY, Chen SP (2014) Occurrence probability and amplitude of equatorial ionospheric irregularities associated with plasma bubbles during low and moderate solar activities (2008–2012). J Geophys Res Space Phys 119:1186–1199. doi:10.1002/2013JA019212

James HG, Parrot M, Berthelier JJ (2012) Very-low-frequency saucers observed on DEMETER. J Geophys Res 117:A09309. doi:10.1029/2012JA017965

Lagoutte D, Berthelier JJ, Lebreton JP, Parrot M, Sauvaud JA (2005) DEMETER microsatellite-scientific mission center-data user guide. DMT-OP-7-CS-6124-LPC v1.0

Lagoutte D, Brochot JY, de Carvalho D, Elie F, Harivelo F, Hobara Y, Madrias L, Parrot M, Pinçon JL, Berthelier JJ, Peschard D, Seran E, Gangloff M, Sauvaud JA, Lebreton JP, Stverak S, Travnicek P, Grygorczuk J, Slominski J, Wronowski R, Barbier S, Bernard P, Gaboriaud A, Wallut JM (2006) The DEMETER science mission centre. Planet Space Sci 54(5):428–440

Lebreton JP, Stverak S, Travnicek P, Maksimovic M, Klinge D, Merikallio S, Lagoutte D, Poirier B, Kozacek Z, Salaquarda M (2006) The ISL Langmuir probe experiment and its data processing onboard DEMETER: scientific objectives, description and first results. Planet Space Sci 54(5):472–486

Lefeuvre F, Blanc E, Pinçon JL, Roussel-Dupré R, Lawrence D, Sauvaud JA, Rauch JL, Feraudy H, Lagoutte D (2008) TARANIS—a satellite project dedicated to the physics of TLEs and TGFs. Space Sci Rev 137:301–315. doi:10.1007/s11214-008-9414-4

Li X, Ma Y, Wang P, Wang H, Lu H, Zhang X, Huang J, Shi F, Yu X, Yanbing X, Meng X, Wang H, Zhao X, Parrot M (2012) Study of the North West Cape electron belts observed by DEMETER satellite. J Geophys Res 117:A04201. doi:10.1029/2011JA017121

Malingre M, Berthelier JJ, Pfaff R, Jasperse J, Parrot M (2008) Lightning-induced lower-hybrid turbulence and trapped extremely low frequency (ELF) electromagnetic waves observed in deep equatorial plasma density depletions during intense magnetic storms. J Geophys Res 113:A11320. doi:10.1029/2008JA013463

Manninen J (2005) Some aspects of ELF–VLF emissions in geophysical research, vol 98. Oulu University Press, Oulu

McIlwain CE (1961) Coordinates for mapping the distribution of magnetically trapped particles. J Geophys Res 66(11):3681–3691

Němec F, Santolík O, Parrot M, Berthelier JJ (2006) Power line harmonic radiation (PLHR) observed by the DEMETER spacecraft. J Geophys Res 111:A04308. doi:10.1029/2005JA011480

Němec F, Santolík O, Parrot M, Berthelier JJ (2007a) Comparison of magnetospheric line radiation and power line harmonic radiation: a systematic survey using the DEMETER spacecraft. J Geophys Res 112:A04301. doi:10.1029/2006JA012134

Němec F, Santolík O, Parrot M, Berthelier JJ (2007b) Power line harmonic radiation: a systematic study using DEMETER spacecraft. Adv Space Res 40(3):398–403. doi:10.1016/j.asr.2007.01.074

Němec F, Santolík O, Parrot M, Bortnik J (2008) Power line harmonic radiation observed by satellite: properties and propagation through the ionosphere. J Geophys Res 113:A08317. doi:10.1029/2008JA013184

Němec F, Parrot M, Santolík O, Rodger CJ, Rycroft MJ, Hayosh M, Shklyar D, Demekhov A (2009a) Survey of magnetospheric line radiation events observed by the DEMETER spacecraft. J Geophys Res 114:A05203. doi:10.1029/2008JA014016

Němec F, Raita T, Parrot M, Santolík O, Turunen T (2009b) Conjugate observations on board a satellite and on the ground of a remarkable MLR-like event. Geophys Res Lett 36:L22103. doi:10.1029/2009GL040974

Němec F, Parrot M, Santolík O (2010) Influence of power line harmonic radiation on the VLF wave activity in the upper ionosphere: is it capable to trigger new emissions? J Geophys Res 115:A11301. doi:10.1029/2010JA015718

Němec F, Parrot M, Santolík O (2012a) Detailed properties of magnetospheric line radiation events observed by the DEMETER spacecraft. J Geophys Res 117:A05210. doi:10.1029/2012JA017517

Němec F, Santolík O, Parrot M, Pickett JS (2012b) Magnetospheric line radiation event observed simultaneously on board Cluster 1, Cluster 2 and DEMETER spacecraft. Geophys Res Lett 39:L18103. doi:10.1029/2012GL053132

Němec F, Santolík O, Parrot M, Pickett JS, Hayosh M, Cornilleau-Wehrlin N (2013) Conjugate observations of quasi-periodic emissions by Cluster and DEMETER spacecraft. J Geophys Res Space Phys 118:1–11. doi:10.1029/2012JA018380

Nunn D, Manninen J, Turunen T, Trakhtengerts V, Erokhin N (1999) On the nonlinear triggering of VLF emissions by power line harmonic radiation. Ann Geophys 17:79–94

Parrot M, Buzzi A, Santolík O, Berthelier JJ, Sauvaud JA, Lebreton JP (2006) New observations of electromagnetic harmonic ELF emissions in the ionosphere by the DEMETER satellite during large magnetic storms. J Geophys Res 111:A08301. doi:10.1029/2005JA011583

Parrot M, Manninen J, Santolík O, Němec F, Turunen T, Raita T, Macúšová E (2007) Simultaneous observation on board a satellite and on the ground of large-scale magnetospheric line radiation. Geophys Res Lett 34:L19102. doi:10.1029/2007GL030630

Parrot M, Inan US, Lehtinen NG (2008a) V-shaped VLF streaks recorded on DEMETER above powerful thunderstorms. J Geophys Res 113:A10310. doi:10.1029/2008JA013336

Parrot M, Santolík O, Brochot JY, Berthelier J-J (2008b) Observation of intensified lower hybrid noise in the midlatitude ionosphere. IEEE Trans Plasma Sci 36(4–1):1164–1165. doi:10.1109/TPS.2008.924492

Parrot M, Němec F, Santolík O (2014a) Statistical analysis of emissions triggered by power line harmonic radiation and observed by the low-altitude satellite DEMETER. J Geophys Res Space Phys 119:5744–5754. doi:10.1002/2014JA020139

Parrot M, Němec F, Santolík O (2014b) Analysis of fine ELF wave structures observed poleward from the ionospheric trough by the low-altitude satellite DEMETER. J Geophys Res Space Phys. doi:10.1002/2013JA019557

Pfaff R, Liebrecht C, Berthelier JJ, Malingre M, Parrot M, Lebreton JP (2008) DEMETER satellite observations of plasma irregularities in the topside ionosphere at low, middle, and sub-auroral latitudes and their dependence on magnetic storms. In Kintner et al (eds) Midlatitude ionospheric dynamics and disturbances, vol 181. AGU Monograph, pp 297–310

Piddyachiy D, Inan US, Bell TF, Lehtinen NG, Parrot M (2008) DEMETER observations of an intense upgoing column of ELF/VLF radiation excited by the HAARP HF heater. J Geophys Res 113:A10308. doi:10.1029/2008JA013208

Píša D (2012) Etude des émissions électromagnétiques enregistrées par le satellite DEMETER. PhD thesis, University of Orléans, October 16, 2012

Rehman MU, Marchand M, Berthelier J-J, Onishi T, Burchill J (2013) Earth magnetic field effects on particle sensors on LEO satellites. IEEE Trans Plasma Sci 41(12):3402–3409

Rodger CJ, Thomson NR, Dowden RL (1995) VLF line radiation observed by satellite. J Geophys Res 100(A4):5681–5689

Rodger CJ, Clilverd MA, Yearby KH, Smith AJ (1999) Magnetospheric line radiation observations at Halley, Antarctica. J Geophys Res 104(A8):17441–17447. doi:10.1029/1999JA900153

Rodger CJ, Clilverd MA, Yearby KH, Smith AJ (2000a) Temporal properties of magnetospheric line radiation. J Geophys Res 105(A1):329–336

Rodger CJ, Clilverd MA, Yearby KH, Smith AJ (2000b) Is magnetospheric line radiation man made? J Geophys Res 105(A7):15981–15990. doi:10.1029/1999JA000413

Santolik O, Parrot M, Chum J (2008) Propagation spectrograms of whistler-mode radiation from lightning. IEEE Trans Plasma Sci 36(4):1166–1167. doi:10.1109/TPS.2008.920899

Santolik O, Parrot M, Inan US, Buresova D, Gurnett DA, Chum J (2009) Propagation of unducted whistlers from their source lightning: a case study. J Geophys Res 114:A03212. doi:10.1029/2008JA013776

Sauvaud JA, Maggiolo R, Jacquey C, Parrot M, Berthelier JJ, Gamble RJ, Rodger CJ (2008) Radiation belt electron precipitation due to VLF transmitters: satellite observations. Geophys Res Lett 35:L09101. doi:10.1029/2008GL033194

Shen X, Zhang X, Wang L, Chen H, Wu Y, Yuan S, Shen J, Zhao S, Qian J, Ding J (2011) The earthquake-related disturbances in ionosphere and project of the first China seismo-electromagnetic satellite. Earthq Sci 24(6):639–650

Shklyar DR, Parrot M, Chum J, Santolik O, Titova EE (2010) On the origin of lower- and upper-frequency cutoffs on wedge-like spectrograms observed by DEMETER in the midlatitude ionosphere. J Geophys Res 115:A05203. doi:10.1029/2009JA014672

Sotnikov VI, Fiala V, Lefeuvre F, Lagoutte D, Mogilevsky M (1991) Excitation of sidebands due to nonlinear coupling between a VLF transmitter signal and a natural ELF emission. J Geophys Res 96(A7):11363–11369

Tanaka Y, Lagoutte D, Hayakawa M, Lefeuvre F, Tajima S (1987) Spectral broadening of VLF transmitter signals and sideband structure observed on Aureol 3 satellite at middle latitudes. J Geophys Res 92(A7):7551–7559

Titova EE, Di VI, Yurov VE, Raspopov OM, Trakhtengertz VYu, Jiricek F, Triska P (1984) Interaction between VLF waves and the turbulent ionosphere. Geophys Res Lett 11(4):323–326

Toledo-Redondo S, Parrot M, Salinas A (2012) Variation of the first cut-off frequency of the Earth-ionosphere waveguide observed by DEMETER. J Geophys Res 117:A04321. doi:10.1029/2011JA017400

Yizengaw E, Retterer J, Pacheco EE, Roddy P, Groves K, Caton R, Baki P (2013) Postmidnight bubbles and scintillations in the quiet-time June solstice. Geophys Res Lett 40:5592–5597. doi:10.1002/2013GL058307